Development of Highly-Efficient ZIF-8@PDMS/PVDF Nanofibrous Composite Membrane for Phenol Removal in Aqueous-Aqueous Membrane Extractive Process

Meng-Yi Jin[1,2†], Yuqing Lin[1†], Yuan Liao[1], Choon-Hong Tan[4], Rong Wang[*,1,3]

1. Singapore Membrane Technology Centre, Nanyang Environment and Water Research Institute, Nanyang Technological University, 1 Cleantech Loop, Singapore 637141, Singapore

2. Interdisciplinary Graduate School, Nanyang Technological University, 50 Nanyang Avenue, Singapore 639798, Singapore

3. School of Civil and Environmental Engineering, Nanyang Technological University, 50 Nanyang Avenue, Singapore 639798, Singapore

4. Department of Chemistry and Biological Chemistry, Nanyang Technological University, 21 Nanyang Link, Singapore 637371, Singapore

† Contribute equally

*Corresponding author at: School of Civil and Environmental Engineering, Nanyang Technological University, 639798 Singapore, Singapore.
Tel.: +65 6790 5327; fax: +65 6791 0676.
E-mail address: rwang@ntu.edu.sg (R. Wang).

Abstract

A highly-efficient zeolitic imidazolate framework-8 (ZIF-8) embedded polydimethylsiloxane (PDMS) mixed matrix membrane (MMM) supported by a polyvinylidene fluoride (PVDF) nanofibrous substrate was developed for phenol removal in an aqueous-aqueous membrane extractive process. Homogeneous nano-scaled dispersion of ZIF-8 in the PDMS matrix was achieved by direct incorporation without intermediate drying process, where the interaction of the randomly-moved nanofillers could be prevented, leading to evenly dispersed ZIF-8 nanofillers and defect-free ZIF-8@PDMS/PVDF nanofibrous composite membranes. The newly-developed ZIF-8@PDMS/PVDF membrane exhibited an exceptionally high overall mass-transfer coefficient, k_0 of 35.7 ± 1.1 × 10^{-7} m/s, doubling that of the pristine membrane in the membrane extractive process. The high performance was maintained for over 360 h without loss of salt rejection. These results could be attributed to the organophilic-assisted "bi-mode" transporting mechanism of ZIF-8 nanofillers in PDMS matrix, namely: (1) the solution-diffusion transport mode; (2) the pore-flow transport mode, where the synergistic effects are expected to significantly improve the phenol transfer efficiency through the membranes. Overall, the results achieved in this work demonstrate promising potential of highly-efficient ZIF-8@PDMS/PVDF nanofibrous composite membranes used for aqueous-aqueous membrane extractive processes for organic-containing wastewater treatments.

Keywords: mixed-matrix membrane; ZIF-8; polydimethylsiloxane; phenol removal, extraction

1. Introduction

Treatment of organic-containing wastewater has drawn increasing attention in recent years [1, 2]. Among the major pollutants, phenol has become a rising concern due to its high toxicity and carcinogenicity, and has been listed as a top priority pollutant by the United States Environmental Protection Agency (US EPA) [3, 4]. On the other hand, phenol is recognized as a valuable chemical for industrial applications such as the production of phenolic resins [5]. Hence, it is of great interest to develop a highly-efficient phenol recovery process from wastewater for environmental sustainability. Existing technologies for phenol treatment include adsorption, solvent extraction, thermal decomposition, biodegradation, oxidation and membrane separation [6, 7]. Among them, the membrane-based aqueous-aqueous extractive process has been evidenced to be a promising technology ascribed to its appealing features, including: (1) the receiving solution can be operated independently under optimized conditions regardless of the wastewater compositions; (2) unlike the centralized classical techniques, the aqueous-aqueous membrane extractive process offers more specific and efficient point-source treatment of individual industrial effluent; (3) it is an energy-saving and cost-effective alternative for phenol recovery due to operation at room temperature and atmospheric pressure [8, 9].

In the aqueous-aqueous membrane extractive process, the target organic compounds are transferred from the feed wastewater to the aqueous receiving solution through a dense membrane based on solution-diffusion mechanism [10]. A variety of receiving solutions such as biological cultures and alkaline solutions can be employed to strip the permeated organics, maintaining the organic concentration driving force imperative for mass transfer across the membrane [11]. Therefore, to a large extent, the aqueous-aqueous extraction efficiency is determined by the mass-transfer capacity of the membrane phase [12]. The ideal characteristics of the dense membrane used for the aqueous-aqueous membrane extractive process should comprise three aspects: (1) high organophilicity to effectively extract the target organics from the aqueous feed; (2) strong hydrophobicity to completely reject water and inorganic components; and (3) low resistance to ensure efficient organic passage. Hence, the design and development of membranes with enhancement in either one or all the aspects are desirable to improve the membrane extractive performance for the targeted organic compounds [13-16]. Cocchini et al. reported an aqueous-aqueous extractive composite

membrane by preparing a 2-μm thick polydimethylsiloxane (PDMS) layer deposited onto microporous polyethersulfone (PES) support. The PDMS/PES composite membrane can achieve the overall mass-transfer coefficient (k_0) of 12 × 10^{-7} m/s [17]. Loh et al. prepared a highly-efficient composite membrane with k_0 of 32 × 10^{-7} m/s, and the membrane transfer resistance could be significantly decreased by reducing the top PDMS layer intrusion into the porous substrate [18]. However, it is worth noting that the reduction of membrane thickness or membrane intrusion not only decreases the membrane resistance, but could also result in membrane defects or weakened mechanical strength for practical applications. Recently, our group developed a condensation-cured PDMS membrane with a quaternary-siloxy-linked three-dimensional network structure [19]. The membrane exhibited high mass-transfer efficiency (k_0 of 18 × 10^{-7} m/s) due to the enhanced PDMS free volume for phenol transport. Therefore, developing new generation membranes with enhanced intrinsic microporosity or free volumes seem to be an effective approach for future study [20].

Incorporating nano-fillers with superior inherent separation properties into polymers to fabricate mixed matrix membranes (MMMs) has been proven to be useful to enhance the membrane performance [21]. Among all types of fillers, metal-organic frameworks (MOFs), comprising inorganic units bridged by organic ligands, are being recognized as one of the most fascinating candidates attributed to their high surface area, large porosity and pore volume, tunable pore size and shape, facile functionalization, and excellent compatibility with polymers [22, 23]. Zeolitic imidazolate framework-8 (ZIF-8), a well-known MOF material, exhibits exceptional chemical and thermal stabilities, as well as strong framework flexibility and hydrophobicity [24]. In the ZIF-8 structure, zinc ions are interconnected by 2-methylimidazole linker molecules forming a sodalite topology with a large accessible cavity of 11.6 Å, connected by small flexible apertures of 3.4 Å [25]. According to literature, ZIF-8 is perceived as a material with intrinsically robust chemical and hydrothermal stabilities, arising from the strong coordination bond between centre metal ions and anionic nitrogen atoms in imidazolate linkers, and the hydrophobic nature with low water uptake capacity [26, 27]. Owing to the flexible nature of ZIF-8 framework, dynamic structural transformations (gate-opening) can take place upon external stimuli such as temperature, pressure and guest molecules [28, 29]. This structural flexibility allows the access of ZIF-8 inner cages by much larger molecules such as 1,2,4-trimethylbenzene whose molecular size (7.6 Å) has been approximated as the limiting aperture size of ZIF-8. Therefore, it is speculated that phenol

molecules (5.1 Å) can transport through the ZIF-8 inner channels, which can serve as expressways with lower mass transfer resistance [30]. Moreover, ZIF-8 can interact with phenol through hydrogen bonding and π-π stacking, which can significantly increase the phenol affinity of the MMM [31]. However, to the best of our knowledge, the use of MOF-incorporated MMMs and their systematic performance study in the aqueous-aqueous membrane extractive process have been rarely reported so far.

The major challenge for synthesizing defect-free and uniform ZIF-8 -based MMMs is the poor dispersion and compatibility between ZIF-8 nanofillers and polymer matrix [32]. Zhang et al. [33] proposed in-situ self-assembly method to prepare ZIF-8/poly sodium 4-styrene-sulfonate (PSS) MMMs, and the uniformly dispersed ZIF-8 based MMMs could be obtained by precisely controlling the coordination bonds between the metal ions (Zn^{2+}) and organic ligands (2-methylimidazole (Hmim)) in every single PSS layer's preparation. Wang et al. [34] prepared MOF-polyimide (PI) MMMs, where the loaded ZIF-8 particles were coated by a layer of polydopamine for improving the interfacial compatibility between MOFs and PI matrix. Although these methods realized good dispersion and compatibility of ZIF-8 in the MMMs, the required pre-treatment of the fillers and/or polymers also simultaneously complicated the overall membrane fabrication procedures and limited their further practical implementations [35, 36]. Additionally, ZIF-8 is an inherently hydrophobic and abundant organic ligand, which favors compatible interface with hydrophobic polymers without surface modification [37]. It has been successfully introduced into hydrophobic polymers such as PSf [38], PPEES [39] and PIM [40], and both enhanced permeability and selectivity were demonstrated. Therefore, one may expect that the well-dispersed ZIF-8 nanofillers could be embedded in PDMS matrix with compatible interface and enhanced permeability/selectivity in aqueous-aqueous membrane extraction process. Therefore, developing simple and conducive methods for the synthesis of defect-free and uniform MMMs with high separation performance is still a scientific and practical challenge.

Herein, a drying-free process to fabricate ZIF-8@PDMS/PVDF nanofibrous composite membrane for phenol removal in the aqueous-aqueous membrane extractive processes was proposed. In this method, the newly-grown ZIF-8 nanofillers were directly introduced into the PDMS solution without intermediate drying process. Under the steric effect of solvent

shell around the newly-grown ZIF-8 nanocrystals, the subsequent interaction and aggregation of the nanofillers could be prevented, thus forming a uniformly distributed ZIF-8@PDMS/PVDF nanofibrous composite membranes, as schematically illustrated in Fig. 1. The resultant membranes were characterized by FESEM, FTIR, XRD and XPS to study the chemico-physical properties, and their phenol separation performances in aqueous-aqueous membrane extraction process were examined to investigate the impact of ZIF-8 nanofillers loading. An organophilic-assisted "bi-mode" transport mechanism was proposed to describe the phenol transport process through the ZIF-8@PDMS/PVDF nanofibrous composite membranes. This study aims to offer an opportunity to exploit the desired characteristics of inorganic and organic materials for fabricating a highly-efficient ZIF-8@PDMS/PVDF nanofibrous composite membranes, for phenol removal from wastewater via the aqueous-aqueous membrane extractive process.

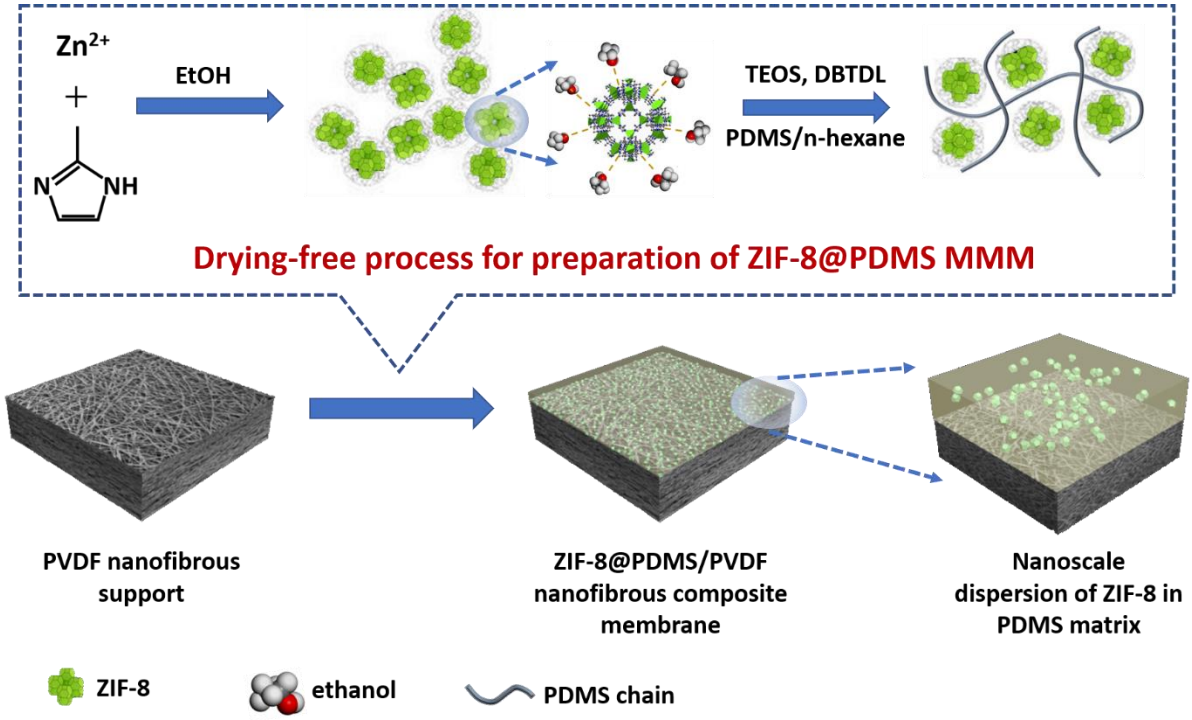

Fig. 1. Schematic illustration of drying-free process for preparation of ZIF-8@PDMS/PVDF nanofibrous composite membranes

2. Experimental

2.1. Materials and chemicals

Polyvinylidene fluoride (PVDF) (Kynar HSV900) was supplied by Arkema and employed as the substrate material. Hydroxyl-terminated polydimethylsiloxane (PDMS, viscosity: 18000-22000 cSt), tetraethyl orthosilicate (TEOS), dibutyltin dilaurate (DBTDL), zinc nitrate hexahydrate (reagent grade, 98%) and 2-methylimidazole (green alternative, 99%) were supplied by Sigma Aldrich. Acetone (Fisher Scientific), *n*-hexane (Merck chemicals), N,N-dimethyl formamide (DMF, Merck chemicals) and ethanol (EMSURE® ACS, ISO, Reag. Ph Eur., Sigma Aldrich) were used as solvents. Glycerol (85% aqueous solution, Merck chemicals) was mixed with deionized water (DI water, purified by a Milli-Q system, Millipore Co. Singapore) to prepare the substrate pre-wetting agent. Sodium chloride (Merck chemicals) and phenol (≥ 99%, Sigma Aldrich) were employed to prepare feed solution. All the reagents were used directly without further treatment.

2.2. Synthesis of ZIF-8 nanofillers

ZIF-8 nanofillers were synthesized following a modified literature procedure [41]. Briefly, a clear solution of $Zn(NO_3)_2 \cdot 6H_2O$ (0.11 g) in ethanol (25 mL) was poured into another clear solution of 2-methylimidazole (Hmim, 2.27 g) in ethanol (50 mL) under stirring, which was continued and stopped after 5 h to produce a homogeneous ZIF-8 suspension. The as-prepared ZIF-8/ethanol suspension was centrifuged and washed with fresh ethanol for three times to remove residues of unreacted reagents and by-products. It was further washed with fresh *n*-hexane and centrifuged for three times in order to enhance the compatibility with the PDMS/*n*-hexane solution. Subsequently, without the drying step, the as-washed ZIF-8 nanofillers were directly re-dispersed in *n*-hexane with a pre-determined concentration for later usage. For comparison, a batch of the as-washed ZIF-8 nanofillers was dried under vacuum at 50 °C overnight (12 h) to afford the pre-formed ZIF-8 nanofillers.

2.3. Preparation of ZIF-8@PDMS MMMs

10 wt% PDMS precursor was first dissolved in *n*-hexane and stirred at room temperature for 1 h. A pre-determined amount of the as-prepared homogeneous ZIF-8/*n*-hexane suspension was transferred into a separate glass bottle, followed by adding the PDMS precursor/*n*-hexane solution dropwise into the container under stirring via a "prime" technique [42]. The mixed ZIF-8/PDMS suspension was stirred vigorously for another 1 h. Subsequently, the cross-linker TEOS (5 wt%) and catalyst DBTDL (1 wt%) were added into the suspension and stirred vigorously for several minutes until the suspension became viscous. The mixture was immediately poured into an aluminum petri dish. Complete solvent evaporation at room

temperature followed by heat cure in an oven at 80 °C for 24 h produced the ZIF-8@PDMS MMM which was peeled off the petri dish for subsequent study. For comparison, the ZIF-8@PDMS MMM with intermediate drying process was also prepared. The major difference was that the collected ZIF-8 nanofillers after drying process (50 °C for 12 h) were added into PDMS precursor/n-hexane solutions, instead of the ZIF-8/n-hexane suspension without intermediate drying process. Moreover, the pristine PDMS dense membrane was also prepared by using the same method without ZIF-8 nanofillers loading. All the resultant ZIF-8@PDMS MMMs and the pristine PDMS dense membrane were 400 ± 30 μm thick, to ensure the nearly same effects of membrane thickness on mass transfer resistance for phenol molecules' transporting.

2.4. Preparation of ZIF-8@PDMS/PVDF nanofibrous composite membranes

A tiered PVDF nanofibrous membrane was fabricated by electrospinning and used as the membrane substrate [10]. The resultant electrospun nanofibrous substrate was pre-wetted by sequential immersion in 80 wt% aqueous ethanol solution, DI water and 75 wt% glycerol aqueous solution (final pre-wetting agent). The pre-wetted substrate was then fixed onto a clean glass plate with tape, while the residual pre-wetting liquid on the substrate surface was quickly removed by a filter paper. Meantime, the coating solution (ZIF-8/PDMS suspension, 5 wt% PDMS) was being prepared following the protocol described above for the MMM fabrication. The coating solution was partially pre-cross-linked to reach an optimum viscosity, in order to ensure a thorough and homogeneous mixing of ZIF-8 nanofillers and PDMS, and to mitigate solution intrusion into the substrate pores upon coating. Subsequently, the partially pre-cross-linked viscous coating solution was spread onto the substrate surface immediately using an automatic film applicator (Elcometer 4340, Elcometer Asia Pte. Ltd.) with a knife height of 50 μm. Evaporation of the solvent residue in a fumehood for 30 min followed by curing in an oven at 80 °C for 24 h afforded the ZIF-8@PDMS/PVDF nanofibrous composite membrane. The resultant composite membrane was detached from the glass plate and immersed in an 80 wt% aqueous ethanol solution (10 min) followed by DI water prior to usage. For comparison, the pristine PDMS/PVDF nanofibrous composite membrane was fabricated in the same way.

2.5. Membrane Characterizations

A field emission scanning electron microscope (FESEM, JSM-7600F, JEOL Asia Pte Ltd, Japan) was employed to observe the surface and cross-sectional morphologies of the samples.

The associated energy dispersive X-ray spectroscopy (EDX) equipment was used to analyze the distribution of ZIF-8 nanofillers in the PDMS matrix as well as the PDMS intrusion degree into the substrate pores. The thickness of the top skin layer of the nanofibrous composite membrane was estimated from the FESEM cross-sectional images. The ZIF-8 particle size distribution in ethanol at 25 °C was measured by a dynamic light scattering (DLS) device (Malvern Zetasizer Nano, DKSH Technology Pte Ltd). X-ray diffraction (XRD) patterns of the ZIF-8 nanofillers and membranes were obtained on a Bruker D8 Advance diffractometer (Cu-Kα X-ray radiation, λ = 1.54 Å) over 5-50° with a 0.02° step size. A Fourier transform infrared (FTIR) spectrophotometer (IRPrestige-21 FTIR, Shimadzu, Japan) was employed to analyze the chemical structures of the ZIF-8 nanofillers (KBr mode: compacted powder tablet, 1 wt% sample + 99 wt% KBr) and membranes (ATR mode: attenuated total reflectance) with a resolution of 4 cm^{-1} and 45 scans. The ZIF-8 nanofillers were dried under vacuum at 50 °C for 24 h prior to XRD and FTIR tests. The chemical composition and states were investigated by X-ray photoelectron spectroscopy (XPS, Thermo ESCALAB 250). The XPS spectrum was analyzed by CasaXPS software, and the C 1s peak with the corrected energy at 284.5 eV was used as the reference for spectral calibration. The morphology of ZIF-8 nanofillers was visualized using field emission transmission electron microscopy (FE-TEM, JEM 2100 F, JEOL) under 200 kV acceleration voltage.

2.6. Aqueous-aqueous membrane extractive experiments

Aqueous-aqueous phenol extractive tests were carried out for the fabricated membranes for 24 h based on a modified procedure [18]. The feed solution comprised 1000 ppm phenol and 5 g/L NaCl in DI water while the receiving solution was DI water. The membranes were mounted into the flat sheet membrane modules with an effective membrane area of 9 cm^2. The phenol mass transfer efficiency was characterized by overall mass transfer coefficient (OMTC), k_0 (m/s), which was calculated by the equation

$$k_0 = (\frac{dC_r}{dt} * V_r)/(A * (C_f - C_r)) \quad (1)$$

where C_r and C_f (g/m^3) were the phenol concentrations at receiving and feed sides respectively at time t (s), V_r (m^3) was the receiving solution volume, and A (m^2) was the effective membrane area.

NaCl flux was recorded to reflect the rejection of water and salts, which was determined by the equation

$$J_s = \Delta c * V/(\Delta t * A) \quad (2)$$

Where J_s (mg/m^2·h) was NaCl flux, Δc (mg/L) was NaCl concentration difference in the receiving solution with volume V (L) during time interval Δt (h), and A (m^2) was the effective membrane area. NaCl concentrations were measured by an inductively coupled plasma optical emission spectrometer (ICP-OES). The feed and permeate chamber volumes of 1 L each were used in this study. The feed and permeate phenol concentrations were measured by high-performance liquid chromatography (HPLC, SHIMADZU, Inertsil OD-3 C18 column) periodically. A plot of phenol concentration against time showed an exponential change of concentration with respect to time for both the feed and permeate sides. Over the initial period of the experiments, the concentration versus time curves were approximately linear and almost levelled off at a longer time.

Long-term aqueous-aqueous phenol extractive tests were conducted for the nanofibrous composite membranes for over 360 h in order to examine the membrane stability. The feed and receiving solutions were refreshed daily to maintain the same phenol concentration gradient during the long-term process.

3. Results and discussion

3.1. Drying-free effect on dispersion of ZIF-8 nanofillers

To demonstrate colloidal stabilities of the ZIF-8 nanofillers, suspensions with and without the drying process, but containing the same amount of ZIF-8 nanofillers were examined for 12 h, as shown in Fig. 2. It could be observed that the phase separation and intrinsic aggregation of ZIF-8 nanofillers after drying process rendered it difficult to obtain a good dispersion. In contrast, for the drying-free ZIF-8 colloidal suspension, the nanofillers could be evenly dispersed for at least 12 h at room temperature, indicating a better colloidal stability with narrower and smaller particle size distribution of 180 nm (**Fig. 2B**). The TEM characterizations of dispersed ZIF-8 nanofillers with and without drying processes were carried out. It could be observed that severe aggregation occurred for the ZIF-8 nanofillers after drying process, forming large particles with an average diameter more than 300 nm, as evidenced by black agglomerates (**Fig. 2C**). The high-resolution TEM image shows a large particle composed of small nanoparticles with clear crystal lattice fringes, further confirming

the successful synthesis of crystalline ZIF-8 particles. For the drying-free ZIF-8 nanofillers, the monodispersed particles with an average diameter of ~20 nm were obtained, further verifying the better colloidal stability with evenly dispersed ZIF-8 nanofillers without aggregation.

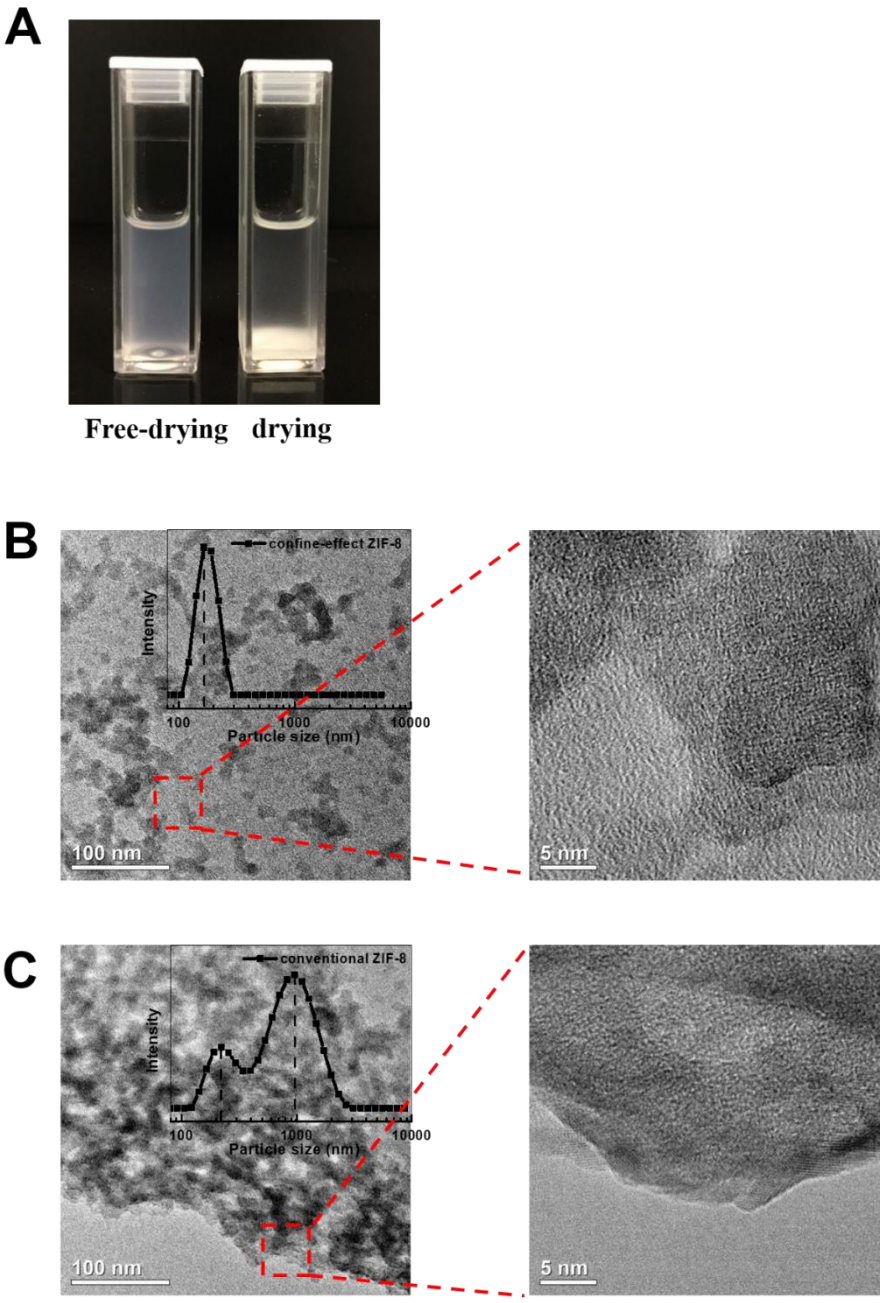

Fig. 2. Characterizations (A) Photo image of ethanol-based ZIF-8 suspensions after 12 h standing prepared by (B) drying-free and (C) conventional drying-redispersion processes.

The better uniformity of the drying-free ZIF-8 colloidal suspension can be explained as follows: the newly-grown ZIF-8 nanofillers are surrounded by solvent shell since nucleation, which prevents interaction and aggregation of the randomly-moved nanoparticles with each other [43]. Conversely, ZIF-8 nanofillers tend to agglomerate during the drying process, and this instability is mainly due to the reaction of Zn-imidazole groups on the surface among themselves, forming strong covalent Zn-imidazole-Zn bonds between the particles during drying process [44, 45]. Moreover, the formed aggregates cannot be easily separated upon subsequent re-dispersion of the nanofillers, resulting in significant agglomeration and sedimentation in the ZIF-8 colloidal suspension prepared by the conventional drying and redispersion process [46]. The good colloidal stability of ZIF-8 suspension prepared in the drying-free process is a critical factor for fabricating a uniform, and defect-free MMMs, which will be discussed in details in section 3.2.

3.2. Chemico-physical characterization of ZIF-8@PDMS MMMs

In order to visually investigate the interfacial interactions between ZIF-8 nanofillers and PDMS matrix, FESEM characterization was carried out on the ZIF-8@PDMS MMMs prepared by drying-free process, with different ZIF-8 nanofillers loadings (0, 1, 4 and 8 wt%), namely ZIF-8@PDMS-0 (pristine PDMS membrane), ZIF-8@PDMS-1, ZIF-8@PDMS-4, and ZIF-8@PDMS-8. As observed in the surface FESEM image (**Fig. 3A**), the pristine PDMS membrane possessed a smooth surface without defect. After adding 1 wt% ZIF-8, the ZIF-8@PDMS-1 MMM with low coverage of ZIF-8 nanofillers wrapped in the PDMS matrix was obtained (**Fig. 3B**). When the ZIF-8 loading was increased to 4 wt%, more ZIF-8 nanofillers were embedded and homogeneously distributed in the PDMS matrix, forming a continuous membrane structure (**Fig. 3C**). Moreover, it should be noting that the nanofillers were almost integrated with the polymer phase without obvious interfacial defects, implying excellent compatibility between ZIF-8 nanofillers and PDMS. The absence of interfacial defects will be further confirmed by the aqueous-aqueous phenol extractive test, as discussed in Section 3.3. However, by incremental addition of ZIF-8 to 8 wt%, micrometer-sized ZIF-8 fillers (1-2 μm) were observed in the membrane (ZIF-8@PDMS-8), as shown in **Fig. 3D**. The formation of large ZIF-8 particles could be attributed to particle aggregation at high ZIF-8 loading, where the probability of particle-particle interaction and collision was increased, leading to more severe particles aggregation in the resultant MMM. In order to further study the drying-free effect on MMM microstructures, the conventional mZIF-8@PDMS-4 MMM prepared with intermediate drying process was also characterized, as shown in **Fig. 3E**. By

comparison with the **Fig. 3C** (ZIF-8@PDMS-4 prepared with the drying-free process), the severe ZIF-8 nanofillers agglomeration, as well as some interfacial defects and cracks along the embedded nanofillers could be observed. The results further proved the drying-free process led to the formation of a homogeneous ZIF-8@PDMS MMMs, possibly due to that the nanoscale and better dispersed ZIF-8 nanofillers enabled good compatibility with PDMS matrix [47, 48]. Moreover, the results also implied that a moderate ZIF-8 nanofillers loading of 4 wt% was optimum for the preparation of uniform ZIF-8@PDMS MMMs, and thus ZIF-8@PDMS-4 MMM was selected for further XRD and FTIR characterizations.

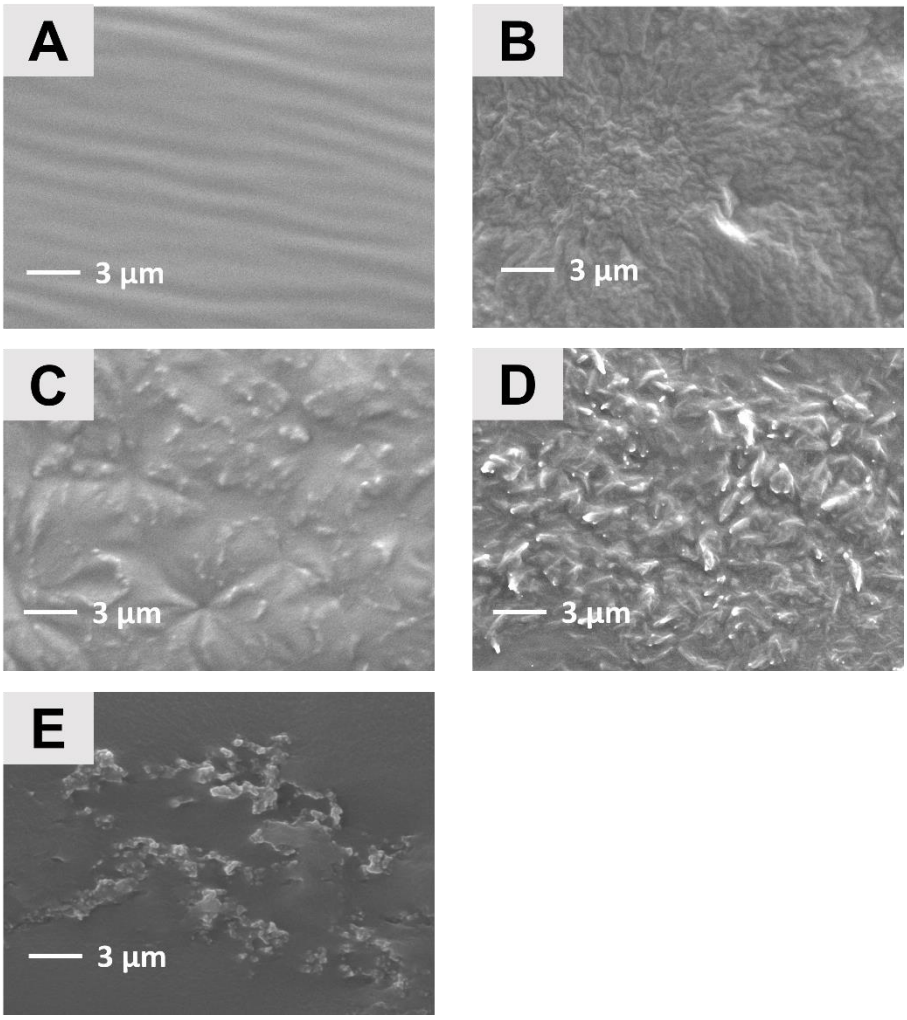

Fig. 3. Surface FESEM images of the ZIF-8@PDMS MMMs prepared without drying process: (A) ZIF-8@PDMS-0 (pristine PDMS membrane); (B) ZIF-8@PDMS-1 (1 wt% ZIF-8); (C) ZIF-8@PDMS-4 (4 wt% ZIF-8),(D) ZIF-8@PDMS-8 (8 wt% ZIF-8) and conventional (E) mZIF-8@PDMS-4 (4 wt% ZIF-8) MMM prepared with intermediate drying process.

As shown in **Fig. 4A,** the XRD pattern confirmed that the synthesized ZIF-8 nanofillers were crystalline, corresponding to a typical sodalite structure [49]. The shift of peak at 2θ of 18.3° in ZIF-8@PDMS-4, relative to the pure ZIF-8 with index (222), could be attributed to the preferential orientation of the nanocrystals in the polymer matrix [50]. In the FTIR pattern of ZIF-8@PDMS-4 (**Fig. 4B**), the signature bands of both ZIF-8 nanofillers and PDMS could be identified. It could be observed that the characteristic peaks of C-H and Si-O stretching vibrations at 1100 and 2964 cm^{-1}, and the characteristic peaks of N-H, C=N and C-N stretching vibrations at 1307, 1580 and 1420 cm^{-1} in ZIF-8@PDMS-4 MMMs were shifted, by comparison with the pure PDMS membrane and ZIF-8 nanofillers, suggesting that chemical interaction had occurred between the incorporated ZIF-8 nanoparticles and PDMS matrix [44]. Moreover, the in-plane bending of the ZIF-8 imidazole ring at 900–1350 cm^{-1} was not well pronounced as it was marked by the strong Si-O-Si bands of PDMS. The results not only illustrated the excellent nanocrystal structure of ZIF-8@PDMS MMMs, but also implied that ZIF-8 incorporation has no adverse influence on the essential structure of the PDMS matrix. In summary, it could be demonstrated that the ZIF-8 nanofillers were well synthesized, and their interaction between ZIF-8 nanofillers and PDMS matrix was favorably conducted.

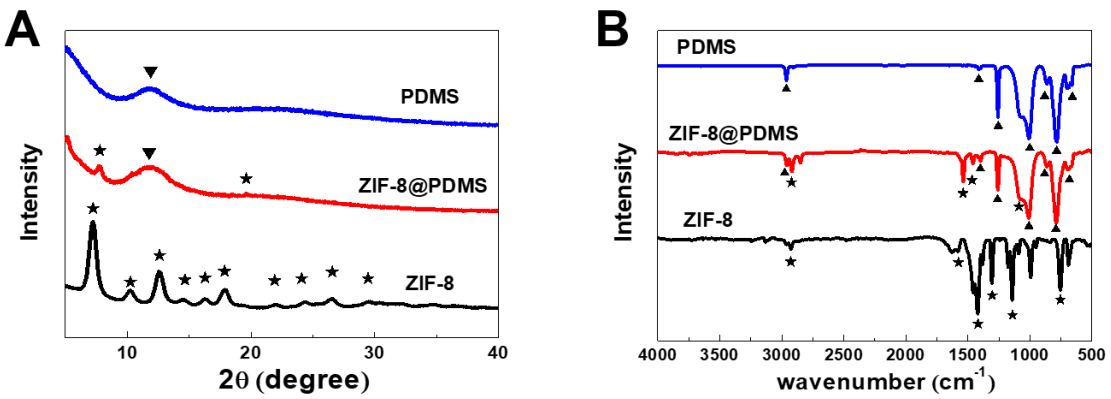

Fig. 4. (A) XRD and (B) FTIR patterns of pristine PDMS membrane, ZIF-8@PDMS-4 and pure ZIF-8 nanocrystals, where the ★ and ▲ representing the characteristic XRD or FTIR peaks of ZIF-8 and PDMS, respectively.

The bonding mechanism of ZIF-8@PDMS MMMs was further confirmed by XPS analysis, as shown in **Fig. 5**. From **Fig. 5A**, no evident signal of Zn element could be detected on the

surface of pristine PDMS membrane. In contrast, for the ZIF-8@PDMS MMMs, the main peak at 1021.7 eV (Zn $2p_{2/3}$) corresponding to Zn^{2+} of the ZIF-8 structure in crystals could be observed [51]. On the other hand, as shown in **Fig. 5B**, the characteristic peak of O 1s consisting of three peaks located at 531.5, 532.0 and 534.0 eV was detected, corresponding to the hydroxyl groups bound to Zn sites (-OH/H_2O), O-Si-O bonds in PDMS polymeric chain, and zinc oxide coordinated with Zn [52]. In the C region (**Fig. 5C**), the main components appeared at 284.4 and 286.2 eV are consistent with the typical C-Si bonds in PDMS, and -CH_3 bonds from the ligand of methylimidazole of ZIF-8 and/or the PDMS matrix [53]. By comparison with the spectra of pristine PDMS membrane, it could be observed that the peak intensity of ZnO and -CH_3 increased, and this was likely due to the coordination of Zn^{2+} and methylimidazole from ZIF-8 with PDMS matrix.

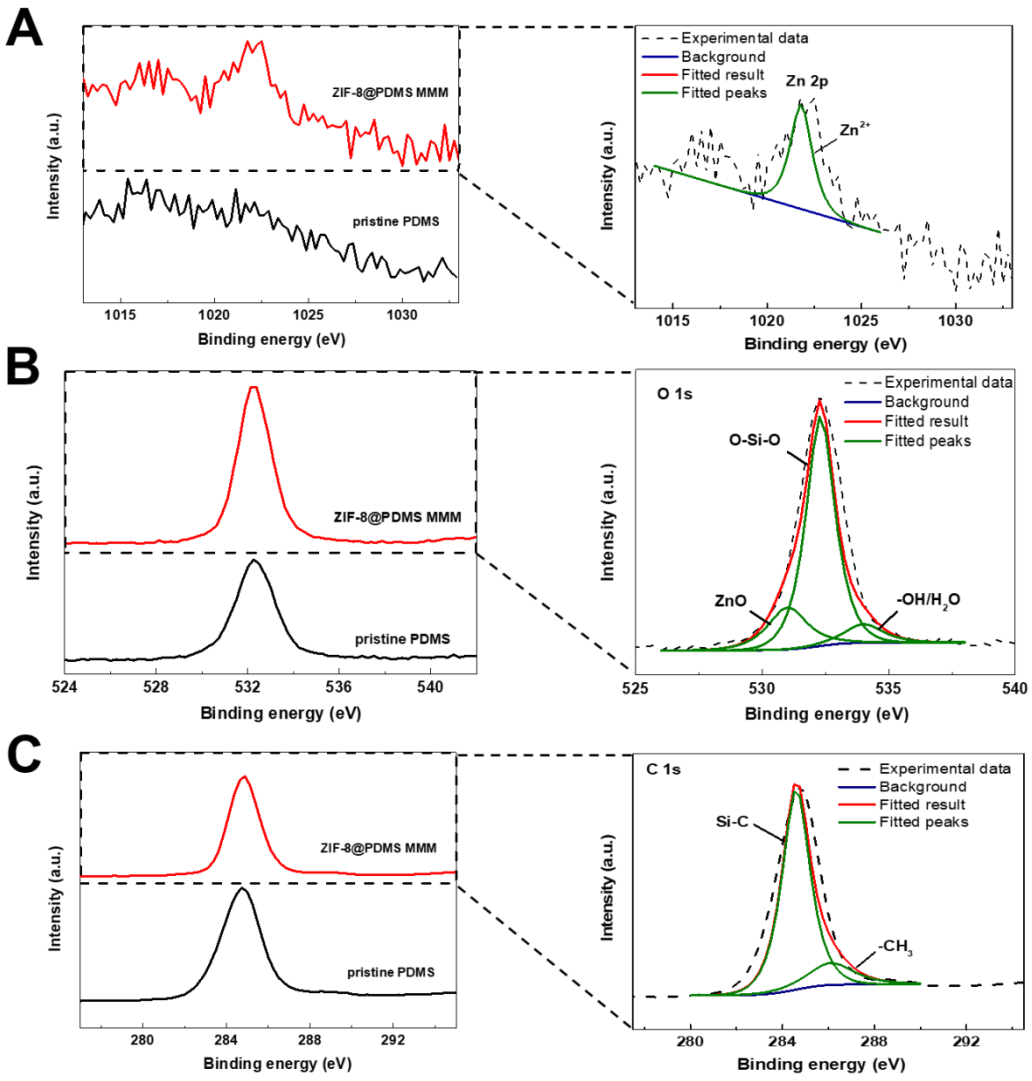

Fig. 5 The XPS characterization of (A) Zn 2p; (B) O 1s; and (C) C 1s on ZIF-8@PDMS-4 MMM and pristine PDMS membrane; and the corresponding curve fittings of ZIF-8@PDMS-4 MMM.

According to the above results, it is believed that the formation of the ZIF-8@PDMS MMM is based on the following mechanism: the inorganic ZIF-8 nanofillers could coordinate with siloxane chains of PDMS via molecular interaction of lone pair electrons from Si-O bonding together with the hydrogen bonding from N-H and -OH from ZnO [32, 54], and finally individually immobilized in polymer PDMS matrix during ZIF-8@PDMS crosslinking and gelation process.

3.3. Aqueous-aqueous membrane extractive performance of ZIF-8@PDMS MMMs

The aqueous-aqueous phenol extractive test was conducted for evaluating the separation performance of ZIF-8@PDMS MMMs (c.a. 400-μm thick) with different ZIF-8 nanofillers loadings (0, 1, 2, 4 and 8 wt%). The phenol extractive performance was determined by the overall mass transfer coefficient (OMTC, k_0) of phenol, while NaCl flux was recorded to reflect the rejection of water and salts. As shown in **Fig. 6**, the k_0 values of the prepared MMMs increased with the increasing of ZIF-8 nanofillers loading amount from 0-4 wt%, while NaCl flux maintained at a negligible level of 8 mg/m^2·h. By comparison with the pristine PDMS membrane (k_0, 1.71 ± 0.04 × 10^{-7} m/s), the ZIF-8@PDMS-4 exhibited a k_0 of 2.61 ± 0.05 × 10^{-7} m/s, showing 53% increment. The negligible and unchanged NaCl flux upon ZIF-8 incorporation (0-4 wt%) indicated the excellent interfacial compatibility between ZIF-8 nanofillers and PDMS matrix without defect, effectively preventing the transport of water molecules and salts through the MMMs [55]. Moreover, according to literature, the effect of ionic strength on the mass transfer of organic permeates could be explained as follows: (1) on one hand, the physical properties such as density and viscosity of the solution, as well as the transport and equilibrium properties such as partition coefficient and diffusion will be altered with the salt concentration. The presence of NaCl will thus mainly affect the resistance in the hydrodynamic boundary layer (HBL) at the membrane surfaces; (2) on the other hand, as phenol is less hydrophobic, the membrane resistance will become dominant over the HBL resistance, contributing mainly to the overall mass transfer resistance [56, 57].

In this study, we incorporated ZIF-8 nanofillers into PDMS matrix for phenol recovery from aqueous NaCl solution, where both ZIF-8 and PDMS matrix are intrinsically hydrophobic in nature, thus the aqueous NaCl does not affect the phenol permeation significantly, especially at a relatively low concentration of 5 g/L in aqueous-aqueous membrane extraction test.

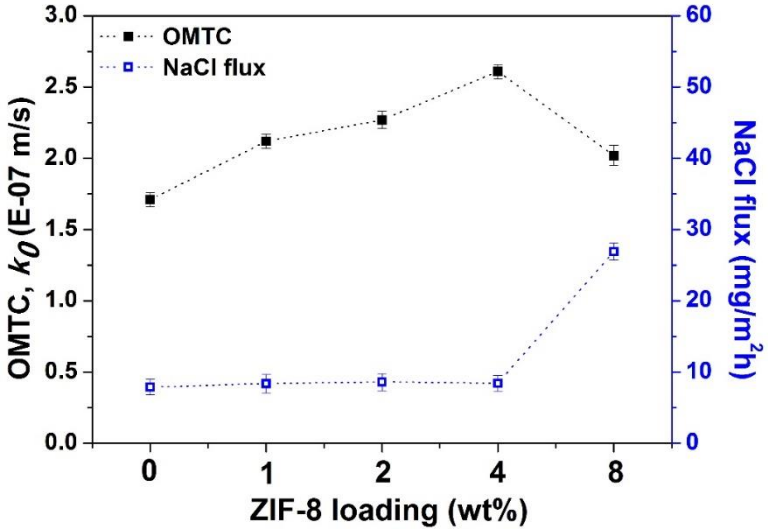

Fig. 6. The effect of ZIF-8 loadings (0, 1, 2, 4 and 8 wt%) on the aqueous-aqueous phenol extractive performance of ZIF-8@PDMS MMMs.

However, when the ZIF-8 doping amount further increased to 8 wt%, a decrease in k_0 (2.02 ± 0.04 × 10^{-7} m/s) and a simultaneous increase in NaCl flux (27 mg/m^2·h) were observed. The deteriorated extractive performance could be attributed to polymer chain rigidification near the PDMS–ZIF-8 interface as well as partial pore blockage of ZIF-8 by PDMS chains at high ZIF-8 loading [58, 59], hampering the solution-diffusion and pore-flow modes for phenol transport. Moreover, significant ZIF-8 aggregates generated in ZIF-8@PDMS-8 (**Fig. 3D**) could promote the formation of microscopic non-selective interfacial voids between ZIF-8 and PDMS, leading to the increased passage of water molecules and salts [60]. Therefore, it could be concluded that a ZIF-8 nanofillers loading of 4 wt% is optimum for fabricating a ZIF-8@PDMS MMM with the highest k_0 and negligible NaCl flux. This optimum MMM formulation will be adopted for the subsequent development of a high-performance ZIF-8@PDMS/PVDF nanofibrous composite membrane for phenol removal in an aqueous-aqueous membrane extractive process.

According to the above results, the organophilic-assisted "bi-mode" transport mechanism could be proposed for phenol transfer through the membrane, as illustrated in **Fig. 7**, namely: (1) a solution-diffusion transport mode is applied in the dense PDMS phase of the MMM (**Fig. 7A**) akin to that in the pristine PDMS membrane [10, 19, 34]. Due to the organophilicity of PDMS, phenol molecules can preferentially transfer through the free volume of the dense PDMS phase where water molecules and salts are essentially retained; (2) a pore-flow transport mode is possible in the microporous ZIF-8 phase of the MMM (**Fig. 7B**) [25]. Although the aperture size of ZIF-8 is estimated to be 3.4 Å, an exceptionally high capacity for phenol molecules (kinetic diameter of 5 Å) was measured for the ZIF-8 nanofillers, indicating a very flexible rather than a rigid framework structure, as shown in Fig. 6. Owing to the structural flexibility of ZIF-8 nanofillers, phenol molecules can access the ZIF-8 nanofillers inner channels via "gate-opening" mechanism [28, 29]. On the other hand, both ZIF-8 and PDMS matrix are intrinsically hydrophobic in nature with low water uptake capacity. In addition, the relatively dense microstructure of ZIF-8 with an aperture size of 3.4 Å implies a very high critical entry pressure for water molecules infiltration. The molecular sieving effect based on hydrophobicity ensures the exclusive passage of phenol molecules through the ZIF-8 cages, while the water molecules were rejected. Therefore, the transfer of the smaller water molecules through the ZIF-8 nanofillers channels is not favored ascribed to the intrinsic hydrophobic nature of ZIF-8 nanofillers inner cages, which supposedly possess much smaller mass transfer resistance than the dense PDMS phase.[25]

Moreover, the organophilic effect is present throughout the entire MMM (**Fig. 7C**). Dense PDMS phase can interact with phenol through hydrogen bonding (O atoms from dimethylsiloxane backbones [$(CH_3)_2$-Si-$O_{2/2}$] and quaternary-siloxy cross-links [Si-$O_{4/2}$] of PDMS with hydroxyl groups [-OH] of phenol) and Van der Waals force (dimethylsiloxane backbones of PDMS with phenyl rings of phenol) [19]. On the other hand, hydrogen bonding (N atoms from imidazole rings of ZIF-8 with hydroxyl groups of phenol) as well as π-π stacking (imidazole rings of ZIF-8 with phenyl rings of phenol) exist between microporous ZIF-8 phase and phenol [31]. The organophilic effect provided by dense PDMS phase and microporous ZIF-8 phase can play a vital role in enhancing the affinity of phenol towards the MMM. Therefore, the organophilic-assisted (1) solution-diffusion and (2) pore-flow modes are expected to significantly improve the phenol transfer efficiency through the ZIF-8@PDMS MMM in comparison with the pristine PDMS membrane where only the solution-

diffusion mechanism is present.

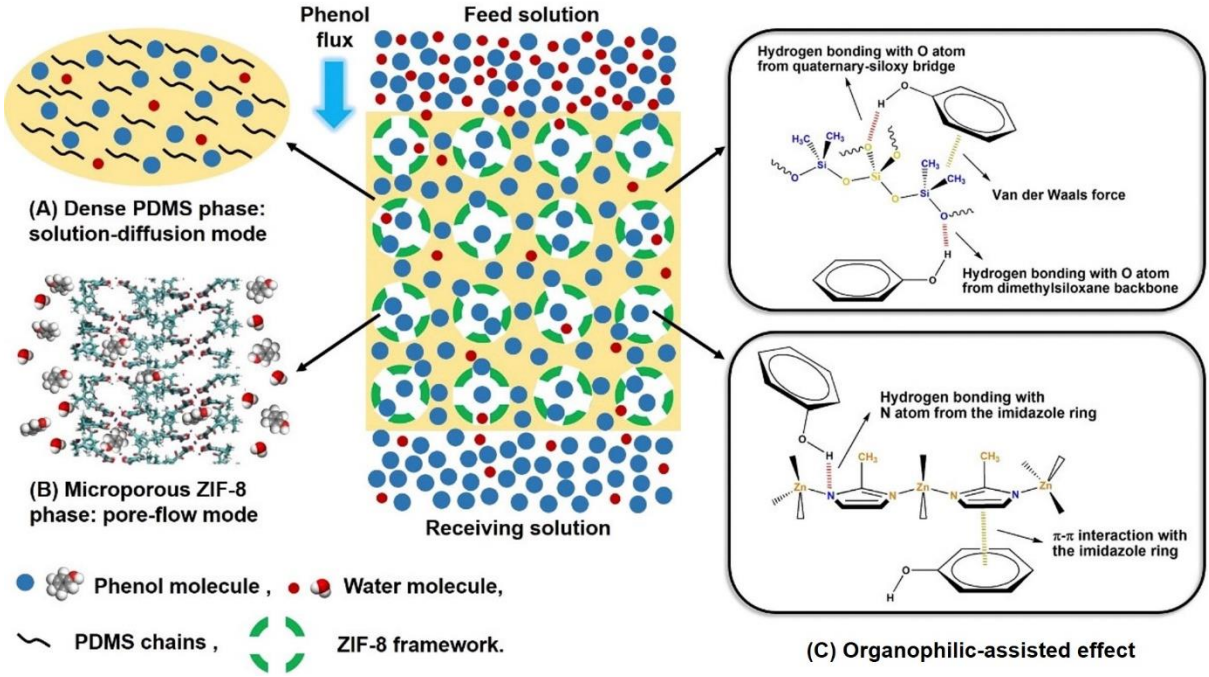

Fig. 7. Schematic diagram of an aqueous-aqueous phenol extractive process based on an organophilic-assisted "bi-mode" transport mechanism for a ZIF-8@PDMS MMM.

3.4. Aqueous-aqueous membrane extractive performance of ZIF-8@PDMS/PVDF nanofibrous composite membranes

We next deposited ZIF-8@PDMS-4 MMMs onto PVDF nanofibrous substrates to further enhance the aqueous-aqueous phenol extraction efficiency in practical application. As observed in the surface FESEM image (**Fig. 8A**), the PVDF electrospun nanofibrous substrate exhibited a highly porous (bulk porosity > 80%) structure with a tightened surface of ultrafine nanofibers (diameter 70 ± 15 nm), which would be beneficial to lower the overall composite membrane resistance significantly [10]. Upon coating by a ZIF-8/PDMS suspension (4 wt% ZIF-8), a uniform and defect-free skin layer was obtained on the top of the nanofibrous support as shown in **Fig. 8B**. The ZIF-8 nanofillers were embedded and distributed uniformly in the PDMS matrix without severe agglomeration, where the results were in accordance with the ZIF-8@PDMS-4 MMM as previously discussed (**Fig. 3C**). As shown in the cross-sectional FESEM image of the ZIF-8@PDMS-4/PVDF nanofibrous composite membrane (**Fig. 8C**), a coherent (c.a. 13 μm) skin layer was formed on the surface of the highly porous nanofibrous support, with ZIF-8 nanofillers embedded in the PDMS matrix. Besides, it could also be observed that the intrusion of the deposited skin layer into

the substrate was well-controlled. This highly intercalated interface further ensured the strong bonding between the ZIF-8@PDMS-4 MMM and PVDF support.

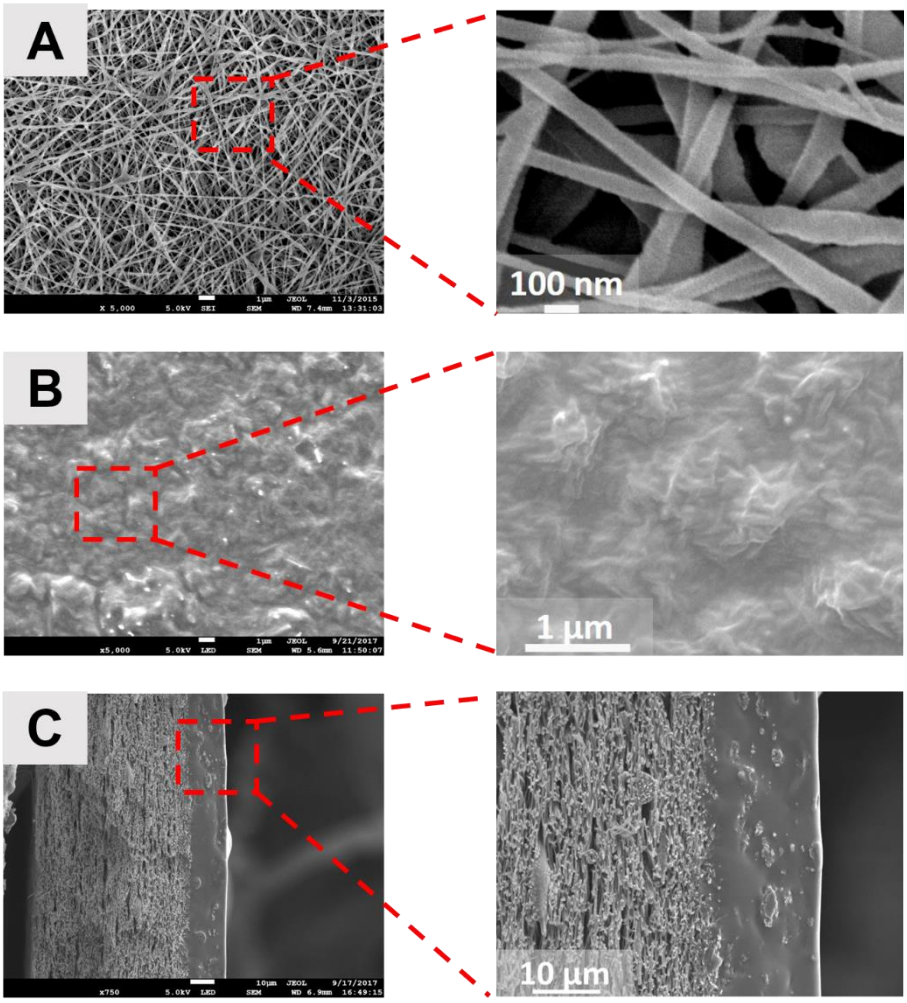

Fig. 8. Surface FESEM images of (A) a tiered PVDF electrospun nanofibrous support; (B) ZIF-8@PDMS-4/PVDF nanofibrous composite membrane M1; and (C) cross-sectional FESEM image of M1.

EDX analyses (**Fig. 9**) were conducted to further examine the ZIF-8 nanofillers distribution in the skin layer of the nanofibrous composite membrane M1. In the surface EDX maps (**Fig. 9A**), the continuous carbon and silicon signals represented the PDMS matrix, while the scattered zinc signal indicated the presence of ZIF-8 nanofillers. The Zn elemental map suggested a homogeneous distribution of ZIF-8 nanofillers on the membrane surface with insignificant aggregation. This was further verified by the cross-sectional EDX analysis of the composite membrane (**Fig. 9B**), where the zinc signal was detected in the skin layer with high uniformity. In addition, silicon was only observed until a depth of c.a. 15 µm from the skin surface, indicating little intrusion of the skin layer into the substrate pores, which also

led to an enhancement in bonding performance for ZIF-8@PDMS-4/PVDF nanofibrous composite membrane.

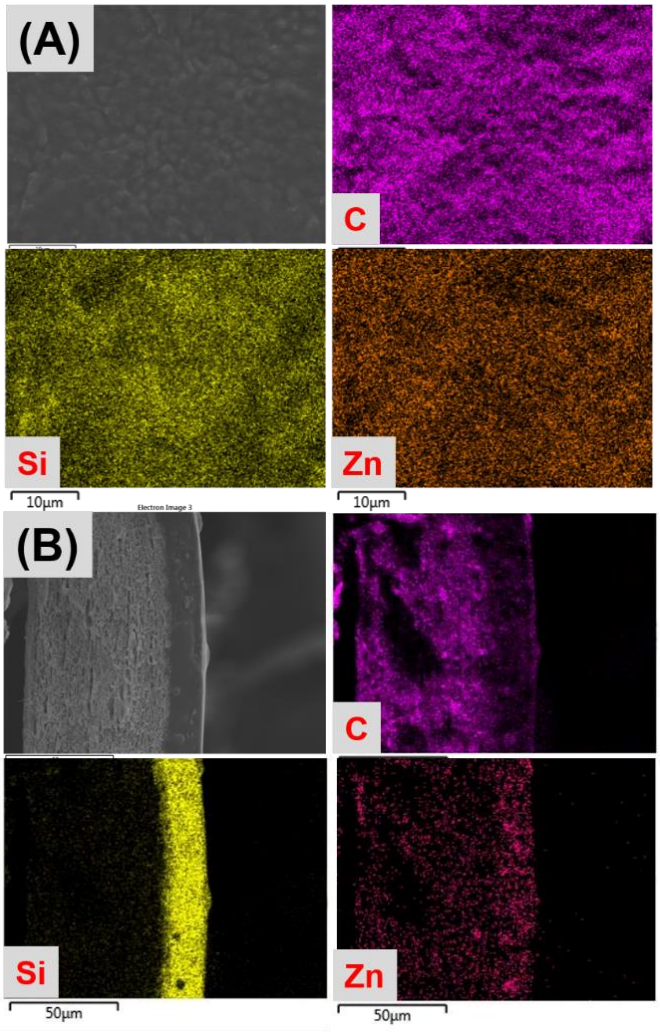

Fig. 9. (A) surface and (B) cross-sectional EDX analyses of ZIF-8@PDMS-4/PVDF nanofibrous composite membrane M1.

When the nanofibrous ZIF-8@PDMS-4/PVDF composite membrane was tested in an aqueous-aqueous phenol extractive process for 24 h, it exhibited an exceptionally high k_0 of 35.7 ± 1.1 × 10^{-7} m/s, doubling that obtained from the pristine counterpart (denoted as M2: k_0, 16.9 ± 1.3 × 10^{-7} m/s) tested under the same operating condition (**Table 1**). Meantime, NaCl flux of composite membrane M1 (12.3 ± 0.4 mg/m^2 h) was maintained at a negligible level similar to M2 (11.8 ± 0.4 mg/m^2 h). This remarkable performance enhancement further demonstrated the superiority of incorporating ZIF-8 nanofillers in the PDMS matrix, and this

could be ascribed to the proposed organophilic-assisted "bi-mode" synergistic transport effect as previously discussed in section 3.3.

Table 1. Aqueous-aqueous phenol extractive performance of nanofibrous composite membranes.

Membrane Code	Skin layer	Skin thickness (μm)	k_0 (E-07m/s)	NaCl flux (mg/m^{2}h)
M1	ZIF-8@PDMS	13.2 ± 1.1	35.7 ± 1.1	12.3 ± 0.4
M2	PDMS	11.8 ± 0.9	16.9 ± 1.3	11.8 ± 0.4

The stability of the developed nanofibrous composite membrane M1 was tested in an aqueous-aqueous phenol extractive process for a prolonged time (> 360 h) and the performance was compared with that of the pristine counterpart M2. As shown in **Fig. 10**, membrane M1 exhibited a steady performance throughout the whole examining period with an average daily k_0 of 36.0 ± 0.3 × 10^{-7} m/s, doubling that obtained from the membrane M2 (16.8 ± 0.2 × 10^{-7} m/s). Meantime, NaCl flux was maintained at a similarly low level (11.6 ± 1.6 mg/m^2·h). This long-term high-performance stability revealed the sound structural integrity of M1 as well as the durability of ZIF-8 as fillers in the PDMS matrix under current testing conditions.

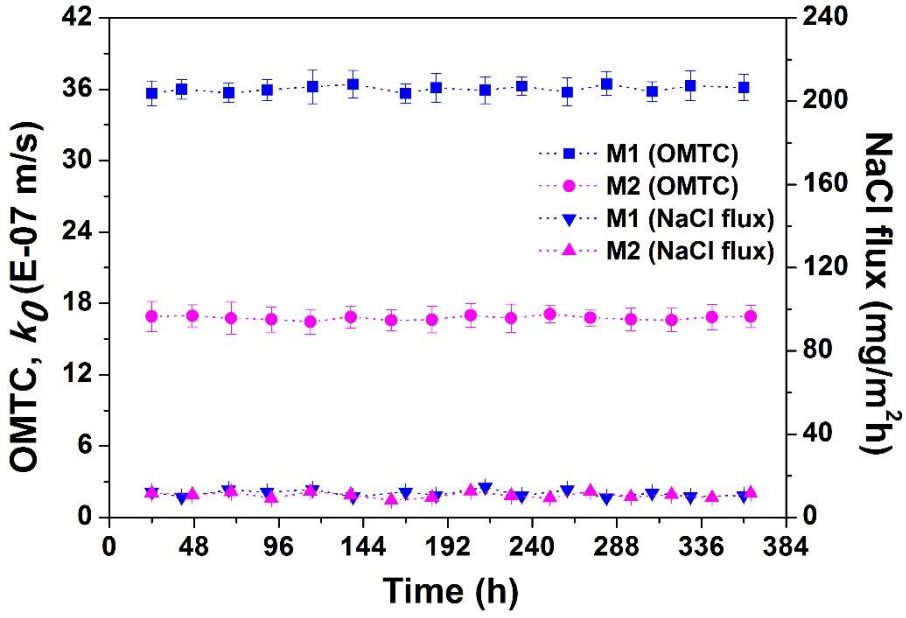

Fig. 10. Long-term performance of the nanofibrous composite membranes M1 and M2.

3.5. Comparison of aqueous-aqueous phenol extractive performance of various membranes

The aqueous-aqueous phenol extractive performance of the newly-developed nanofibrous composite membrane M1 was compared with that of a commercial tubular silicone rubber membrane, PDMS-based TFC membranes and PDMS-coated PVDF nanofibrous composite membranes developed in our previous studies, as shown in **Table 2**. For all the works cited in this table, the permeate chambers were filled with water, similar to the condition used in the aqueous-aqueous phenol extraction test in this study. It could be seen that the composite membrane M1 developed in this work outperformed most of the precedent membranes in terms of phenol overall mass transfer coefficient, showing the enhanced performance of phenol removal in an aqueous-aqueous membrane extractive process up to date. The remarkable performance enhancement indicated that the resultant ZIF-8@PDMS/PVDF nanofibrous composite membranes could be promising to be applied in aqueous-aqueous membrane extractive processes to remove other types of organic pollutants.

Table 2. Comparison of aqueous-aqueous phenol extractive performance of various membranes.

Membrane type	**PDMS thickness (μm)**	**Substrate pore size (μm)**	**Feed solution condition**	**Reynolds number**	**OMTC, k_0 (E-07 m/s)**	**Reference**
#1 Tubular silicone rubber membrane	500	N.A.	1000 ppm phenol solution	12000 (feed side) 4700 (receiving side)	1.0	[14], 1995
#2 Tubular silicone rubber membrane	250	N.A.	1000 ppm phenol solution	12000 (feed side) 4700 (receiving side)	1.7	[14], 1995
#3 PDMS/PES TFC tubular membrane	2	0.1-10	phenol solution	7500 (feed side) 2700 (receiving side)	12	[17], 2002
#4 PDMS/PEI TFC-HF membrane	0.5-2	0.05	1000 ppm phenol, 50 g/L NaCl	1000 (both sides)	32	[18], 2016
#5 PDMS/PVDF nanofibrous composite membrane	55	0.3-0.6	1000 ppm phenol, 1 M HCl, 50 g/L NaCl	400 (both sides)	9.3	[10], 2017
#6 PDMS/PVDF nanofibrous composite membrane	7	0.3-0.6	1000 ppm phenol, 5 g/L NaCl	270 (both sides)	18	[19], 2018
#7 ZIF-8@PDMS/PVDF nanofibrous composite membrane	13	0.3-0.6	1000 ppm phenol, 5 g/L NaCl	300 (both sides)	36	Current work

4. Conclusions

A highly-efficient ZIF-8@PDMS/PVDF nanofibrous composite membrane was designed and fabricated by direct incorporation with the drying-free process for phenol removal in an aqueous-aqueous membrane extractive process. The nanoscaled dispersion of ZIF-8 nanofillers distributed throughout the PDMS matrix could be obtained via the drying-free process. The newly-developed nanofibrous composite membrane exhibited a remarkable k_0 of $35.7 \pm 1.1 \times 10^{-7}$ m/s in an aqueous-aqueous phenol extractive test, and the high extractive performance was maintained for more than 360 h without a drop in salt rejection. The appealing outcome was believed to be realized by organophilic-assisted "bi-mode" synergistic effects, namely: (1) the solution-diffusion, (2) the pore-flow modes for phenol molecules favorably passing through the ZIF-8@PDMS/PVDF nanofibrous composite membranes. The drying-free strategy for incorporating filler materials in the polymer matrix has contributed to the development of high-performance ZIF-8@PDMS/PVDF nanofibrous composite membranes for diverse membrane separation processes.

Acknowledgments

This research grant is supported by the Singapore National Research Foundation under its Environmental & Water Technologies Strategic Research Programme and administered by the Environment & Water Industry Programme Office (EWI) of the PUB (EWI RFP 1102-IRIS-02-03). We acknowledge funding support from the Singapore Economic Development Board to the Singapore Membrane Technology Centre (SMTC). We also appreciate the comments and advice provided by Professor Tony Fane from SMTC.

References

[1] B.J.L. Yeo, S. Goh, J. Zhang, A.G. Livingston, A.G. Fane, Novel MBRs for the removal of organic priority pollutants from industrial wastewaters: a review, J. Chem. Technol. Biotechnol., 90 (2015) 1949-1967.

[2] Y. Liao, C.H. Loh, M. Tian, R. Wang, A.G. Fane, Progress in electrospun polymeric nanofibrous membranes for water treatment: Fabrication, modification and applications, Prog. Polym. Sci., 77 (2018) 69-94.

[3] V.C. Srivastava, M.M. Swamy, I.D. Mall, B. Prasad, I.M. Mishra, Adsorptive removal of phenol by bagasse fly ash and activated carbon: Equilibrium, kinetics and thermodynamics, Coll. Surfs. a-Physchem. Eng. Asps., 272 (2006) 89-104.

[4] Toxicological Profile for Phenol, Agency for Toxic Substances and Disease Registry (ATSDR), US Department of Health and Human Services, Public Health Service, Atlanta, Georgia, (1998).

[5] A.A. Peyghan, M.T. Baei, M. Moghimi, S. Hashemian, Phenol adsorption study on pristine, Ga-, and In-doped (4, 4) armchair single-walled boron nitride nanotubes, Comput. Theor. Chem., 997 (2012) 63-69.

[6] L.G.C. Villegas, N. Mashhadi, M. Chen, D. Mukherjee, K.E. Taylor, N. Biswas, A short review of techniques for phenol removal from wastewater, Curr. Pollut. Rep., 2 (2016) 157-167.

[7] Y. Liao, M. Tian, S. Goh, R. Wang, A.G. Fane, Effects of internal concentration polarization and membrane roughness on phenol removal in extractive membrane bioreactor, J. Membr. Sci., 563 (2018) 309-319.

[8] A.G. Livingston, A novel membrane bioreactor for detoxifying industrial wastewater: I. biodegradation of phenol in a synthetically concocted wastewater, Biotechnol. Bioeng., 41 (1993) 915-926.

[9] Y. Liao, S.W. Goh, M. Tian, R. Wang, A.G. Fane, Design, development and evaluation of nanofibrous composite membranes with opposing membrane wetting properties for extractive membrane bioreactors, J. Membr. Sci., 551 (2018) 55-65.

[10] M.-Y. Jin, Y. Liao, C.H. Loh, C.-H. Tan, R. Wang, Preparation of polydimethylsiloxane–polyvinylidene fluoride composite membranes for phenol removal in extractive membrane bioreactor, Ind. Eng. Chem. Res., 56 (2017) 3436-3445.

[11] J. Sawai, N. Ito, T. Minami, M. Kikuchi, Separation of low volatile organic compounds, phenol and aniline derivatives, from aqueous solution using silicone rubber membrane, J. Membr. Sci., 252 (2005) 1-7.
[12] V. Chavan, S. Paul, A.K. Pandey, P.C. Kalsi, A. Goswami, Thin extractive membrane for monitoring actinides in aqueous streams, J. Hazard. Mater., 260 (2013) 53-60.
[13] P.R. Brookes, A.G. Livingston, Point source detoxification of an industrially produced 3,4-dichloroaniline-manufacture wastewater using a membrane bioreactor, Appl. Microbiol. Biotechnol., 39 (1993) 764-771.
[14] P.R. Brookes, A.G. Livingston, Aqueous-aqueous extraction of organic pollutants through tubular silicone rubber membranes, J. Membr. Sci., 104 (1995) 119-137.
[15] U. Cocchini, C. Nicolella, A.G. Livingston, Braided silicone rubber membranes for organic extraction from aqueous solutions I. mass transport studies, J. Membr. Sci., 199 (2002) 85-99.
[16] E.A.C. Emanuelsson, J.P. Arcangeli, A.G. Livingston, The anoxic extractive membrane bioreactor, Water Res., 37 (2003) 1231-1238.
[17] U. Cocchini, C. Nicolella, A.G. Livingston, Countercurrent transport of organic and water molecules through thin film composite membranes in aqueous-aqueous extractive membrane processes. part I: experimental characterisation, Chem. Eng. Sci., 57 (2002) 4087-4098.
[18] C.H. Loh, Y. Zhang, S. Goh, R. Wang, A.G. Fane, Composite hollow fiber membranes with different poly(dimethylsiloxane) intrusions into substrate for phenol removal via extractive membrane bioreactor, J. Membr. Sci., 500 (2016) 236-244.
[19] M.-Y. Jin, Y. Liao, C.-H. Tan, R. Wang, Development of high performance nanofibrous composite membranes by optimizing polydimethylsiloxane architectures for phenol transport, J. Membr. Sci., 549 (2018) 638-648.
[20] H.B. Park, C.H. Jung, Y.M. Lee, A. J. Hill, S.J. Pas, S.T. Mudie, E.V. Wagner, B.D. Freeman, D.J. Cookson, Polymers with cavities tuned for fast selective transport of small molecules and ions, Science, 318 (2007) 254-258.
[21] T.-S. Chung, L.Y. Jiang, Y. Li, S. Kulprathipanja, Mixed matrix membranes (MMMs) comprising organic polymers with dispersed inorganic fillers for gas separation, Prog. Polym. Sci., 32 (2007) 483-507.
[22] H. Furukawa, K.E. Cordova, M. O'Keeffe, O.M. Yaghi, The chemistry and applications of metal-organic frameworks, Science, 341 (2013) 1230444.

[23] H.-C. Zhou, J.R. Long, O.M. Yaghi, Introduction to metal-organic frameworks, Chem. Rev., 112 (2012) 673-674.
[24] S.R. Venna, M.A. Carreon, Highly Permeable Zeolite Imidazolate Framework-8 Membranes for CO2/CH4 Separation, J. Am. Chem. Soc., 132 (2010) 76-+.
[25] K. Zhang, R.P. Lively, C. Zhang, R.R. Chance, W.J. Koros, D.S. Sholl, S. Nair, Exploring the framework hydrophobicity and flexibility of ZIF-8: from biofuel recovery to hydrocarbon separations, J. Phys. Chem. Lett. , 4 (2013) 3618-3622.
[26] H. Zhang, D. Liu, Y. Yao, B. Zhang, Y.S. Lin, Stability of ZIF-8 membranes and crystalline powders in water at room temperature, J. Membr. Sci., 485 (2015) 103-111.
[27] H. Zhang, J. James, M. Zhao, Y. Yao, Y. Zhang, B. Zhang, Y.S. Lin, Improving hydrostability of ZIF-8 membranes via surface ligand exchange, J. Membr. Sci., 532 (2017) 1-8.
[28] D. Fairen-Jimenez, S.A. Moggach, M.T. Wharmby, P.A. Wright, S. Parsons, T. Duren, Opening the gate: framework flexibility in ZIF-8 explored by experiments and simulations, J. Am. Chem. Soc., 133 (2011) 8900-8902.
[29] S.M. Hyun, J.H. Lee, G.Y. Jung, Y.K. Kim, T.K. Kim, S. Jeoung, S.K. Kwak, D. Moon, H.R. Moon, Exploration of gate-opening and breathing phenomena in a tailored flexible metal-organic framework, Inorg. Chem., 55 (2016) 1920-1925.
[30] T. Atoguchi, T. Kanougi, T. Yamamoto, S. Yao, Phenol oxidation into catechol and hydroquinone over H-MFI, H-MOR, H-USY and H-BEA in the presence of ketone, J. Mol. Catal. A: Chem., 220 (2004) 183-187.
[31] M.T. Luebbers, T. Wu, L. Shen, R.I. Masel, Effects of molecular sieving and electrostatic enhancement in the adsorption of organic compounds on the zeolitic imidazolate framework ZIF-8, Langmuir : the ACS journal of surfaces and colloids, 26 (2010) 15625-15633.
[32] H. Fan, Q. Shi, H. Yan, S. Ji, J. Dong, G. Zhang, Simultaneous spray self-assembly of highly loaded ZIF-8-PDMS nanohybrid membranes exhibiting exceptionally high biobutanol-permselective pervaporation, Angew. Chem. Int. Ed. Engl., 53 (2014) 5578-5582.
[33] R. Zhang, S. Ji, N. Wang, L. Wang, G. Zhang, J.R. Li, Coordination-driven in situ self-assembly strategy for the preparation of metal-organic framework hybrid membranes, Angew. Chem. Int. Ed., 53 (2014) 9775-9779.
[34] Z. Wang, D. Wang, S. Zhang, L. Hu, J. Jin, Interfacial design of mixed matrix membranes for improved gas separation performance, Adv. Mater., 28 (2016) 3399-3405.

[35] J. Dechnik, J. Gascon, C.J. Doonan, C. Janiak, C.J. Sumby, Mixed-matrix membranes, Angew. Chem. Int. Ed., 56 (2017) 9292-9310.
[36] T. Kitao, Y. Zhang, S. Kitagawa, B. Wang, T. Uemura, Hybridization of MOFs and polymers, Chem. Soc. Rev., 46 (2017) 3108-3133.
[37] M. Fang, C. Wu, Z. Yang, T. Wang, Y. Xia, J. Li, ZIF-8/PDMS mixed matrix membranes for propane/nitrogen mixture separation: Experimental result and permeation model validation, J. Membr. Sci., 474 (2015) 103-113.
[38] B. Zornoza, B. Seoane, J.M. Zamaro, C. Tellez, J. Coronas, Combination of MOFs and Zeolites for Mixed-Matrix Membranes, Chemphyschem, 12 (2011) 2781-2785.
[39] K. Diaz, M. Lopez-Gonzalez, L.F. del Castillo, E. Riande, Effect of zeolitic imidazolate frameworks on the gas transport performance of ZIF8-poly(1,4-phenylene ether-ether-sulfone) hybrid membranes, J. Membr. Sci., 383 (2011) 206-213.
[40] A.F. Bushell, M.P. Attfield, C.R. Mason, P.M. Budd, Y. Yampolskii, L. Starannikova, A. Rebrov, F. Bazzarelli, P. Bernardo, J.C. Jansen, M. Lanc, K. Friess, V. Shantarovich, V. Gustov, V. Isaeva, Gas permeation parameters of mixed matrix membranes based on the polymer of intrinsic microporosity PIM-1 and the zeolitic imidazolate framework ZIF-8, J. Membr. Sci., 427 (2013) 48-62.
[41] J. Cravillon, R. Nayuk, S. Springer, A. Feldhoff, K. Huber, M. Wiebcke, Controlling zeolitic imidazolate framework nano-and microcrystal formation: insight into crystal growth by time-resolved in situ static light scattering, Chem. Mater., 23 (2011) 2130-2141.
[42] G. Dong, H. Li, V. Chen, Challenges and opportunities for mixed-matrix membranes for gas separation, J. Mater. Chem. A., 1 (2013) 4610.
[43] Y.-H. Deng, J.-T. Chen, C.-H. Chang, K.-S. Liao, K.-L. Tung, W.E. Price, Y. Yamauchi, K.C.W. Wu, A drying-free, water-based process for fabricating mixed-matrix membranes with outstanding pervaporation performance, Angew. Chem. Int. Ed., 55 (2016) 12793-12796.
[44] Z. Wang, D. Wang, S. Zhang, L. Hu, J. Jin, Interfacial Design of Mixed Matrix Membranes for Improved Gas Separation Performance, Adv. Mater., 28 (2016) 3399-3405.
[45] H. Fan, N. Wang, S. Ji, H. Yan, G. Zhang, Nanodisperse ZIF-8/PDMS hybrid membranes for biobutanol permselective pervaporation, J. Mater. Chem. A, 2 (2014) 20947-20957.
[46] A. Razmjou, J. Mansouri, V. Chen, The effects of mechanical and chemical modification of TiO2 nanoparticles on the surface chemistry, structure and fouling performance of PES ultrafiltration membranes, J. Membr. Sci., 378 (2011) 73-84.

[47] J. Zhu, L. Qin, A. Uliana, J. Hou, J. Wang, Y. Zhang, X. Li, S. Yuan, J. Li, M. Tian, J. Lin, B. Van der Bruggen, Elevated Performance of Thin Film Nanocomposite Membranes Enabled by Modified Hydrophilic MOFs for Nanofiltration, ACS Appl Mater Interfaces, 9 (2017) 1975-1986.
[48] Y.H. Deng, J.T. Chen, C.H. Chang, K.S. Liao, K.L. Tung, W.E. Price, Y. Yamauchi, K.C.W. Wu, A Drying-Free, Water-Based Process for Fabricating Mixed-Matrix Membranes with Outstanding Pervaporation Performance, Angewandte Chemie-International Edition, 55 (2016) 12793-12796.
[49] K.S. Park, Z. Ni, A.P. Cote, J.Y. Choi, R. Huang, F.J. Uribe-Romo, H.K. Chae, M. O'Keeffe, O.M. Yaghi, Exceptional chemical and thermal stability of zeolitic imidazolate frameworks, Proc. Natl. Acad. Sci. U.S.A., 103 (2006) 10186-10191.
[50] J.W. Hou, P.D. Sutrisna, Y.T. Zhang, V. Chen, Formation of ultrathin, continuous metal-organic framework membranes on flexible polymer substrates (XRD), Angew. Chem. Int. Ed., 55 (2016) 3947-3951.
[51] Q. Guo, C. Chen, L. Zhou, X. Li, Z. Li, D. Yuan, J. Ding, H. Wan, G. Guan, Design of ZIF-8/ion copolymer hierarchically porous material: Coordination effect on the adsorption and diffusion for carbon dioxide, Microporous Mesoporous Mater., 261 (2018) 79-87.
[52] F. Tian, A.M. Cerro, A.M. Mosier, H.K. Wayment-Steele, R.S. Shine, A. Park, E.R. Webster, L.E. Johnson, M.S. Johal, L. Benz, Surface and Stability Characterization of a Nanoporous ZIF-8 Thin Film, The Journal of Physical Chemistry C, 118 (2014) 14449-14456.
[53] R. Dahiya, G. Gottardi, N. Laidani, PDMS residues-free micro/macrostructures on flexible substrates, Microelectron. Eng., 136 (2015) 57-62.
[54] E. Barankova, N. Pradeep, K.V. Peinemann, Zeolite-imidazolate framework (ZIF-8) membrane synthesis on a mixed-matrix substrate, Chem Commun (Camb), 49 (2013) 9419-9421.
[55] X.L. Liu, Y.S. Li, G.Q. Zhu, Y.J. Ban, L.Y. Xu, W.S. Yang, An organophilic pervaporation membrane derived from metal-organic framework nanoparticles for efficient recovery of bio-alcohols, Angew. Chem. Int. Ed., 50 (2011) 10636-10639.
[56] U. Cocchini, C. Nicolella, A.G. Livingston, Countercurrent transport of organic and water molecules through thin film composite membranes in aqueous-aqueous extractive membrane processes. Part I: experimental characterisation, Chem. Eng. Sci., 57 (2002) 4087-4098.
[57] U. Cocchini, C. Nicolella, A.G. Livingston, Effect of ionic strength on extraction of hydrophobic organics through silicone rubber membranes, J. Membr. Sci., 162 (1999) 57-72.

[58] Y. Li, T. Chung, C. Cao, S. Kulprathipanja, The effects of polymer chain rigidification, zeolite pore size and pore blockage on polyethersulfone (PES)-zeolite A mixed matrix membranes, J. Membr. Sci., 260 (2005) 45-55.
[59] T.T. Moore, R. Mahajan, D.Q. Vu, W.J. Koros, Hybrid membrane materials comprising organic polymers with rigid dispersed phases, AlChE J., 50 (2004) 311-321.
[60] J.-T. Chen, C.-C. Shih, Y.-J. Fu, S.-H. Huang, C.-C. Hu, K.-R. Lee, J.-Y. Lai, Zeolite-filled porous mixed matrix membranes for air separation, Ind. Eng. Chem. Res., 53 (2014) 2781-2789.

Fig. 1

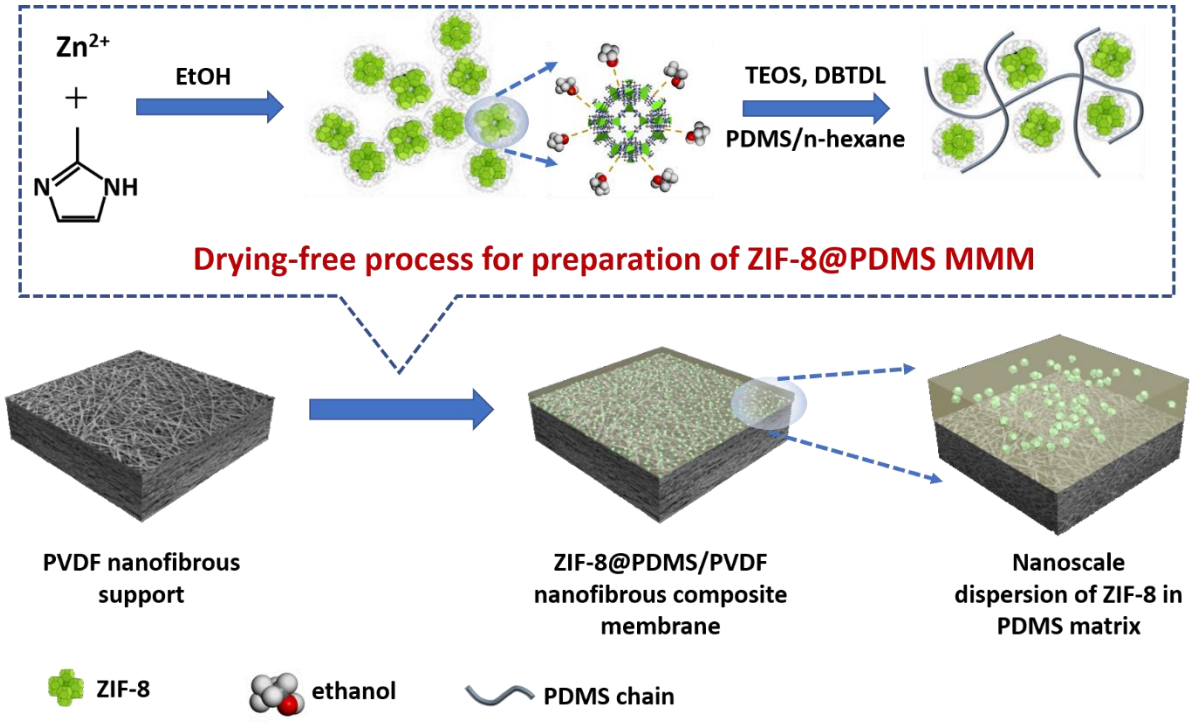

Fig. 1. Schematic illustration of drying-free process for preparation of ZIF-8@PDMS/PVDF nanofibrous composite membranes.

Fig. 2

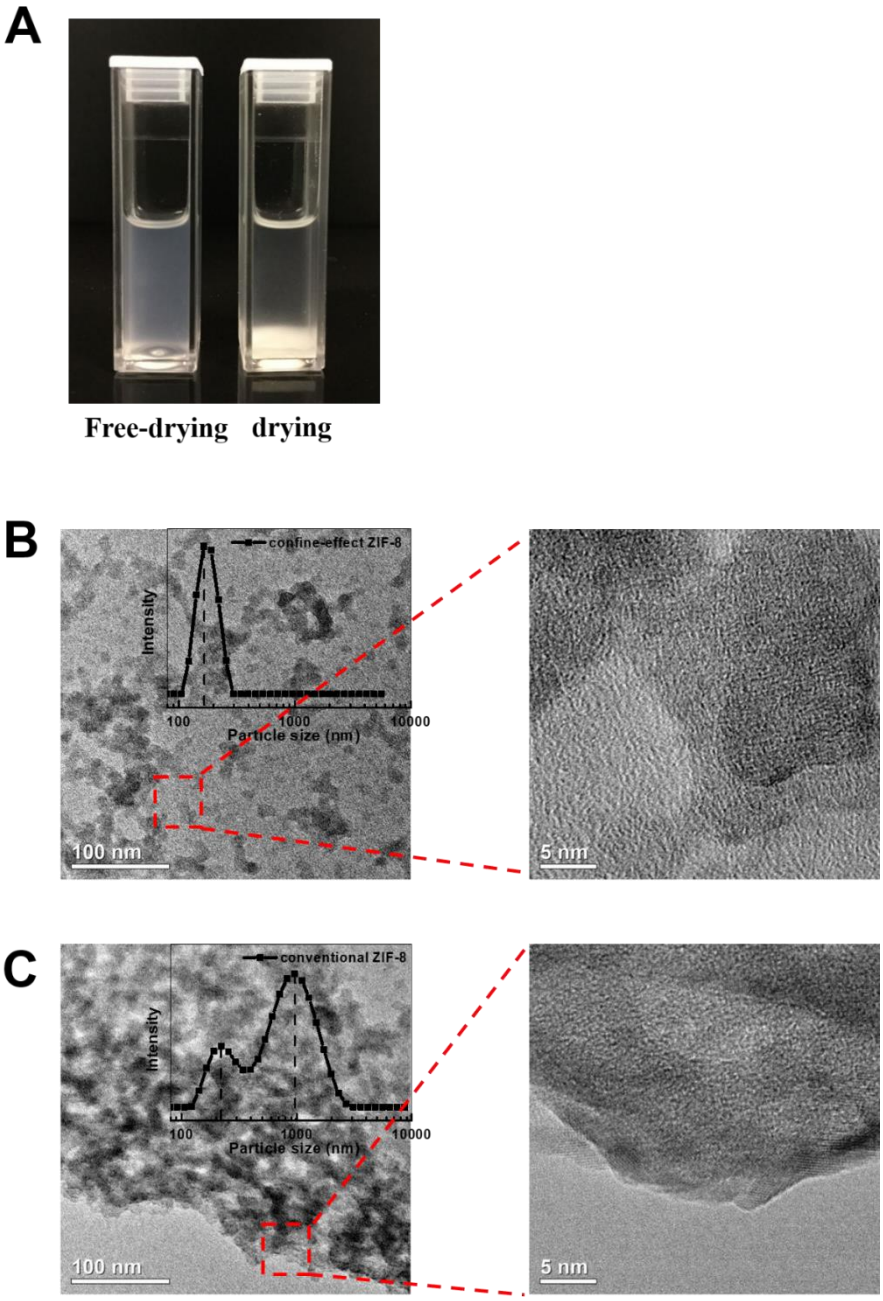

Fig. 2. Characterizations (A) Photo image of ethanol-based ZIF-8 suspensions after 12 h standing prepared by (B) drying-free and (C) conventional drying-redispersion processes.

Fig. 3

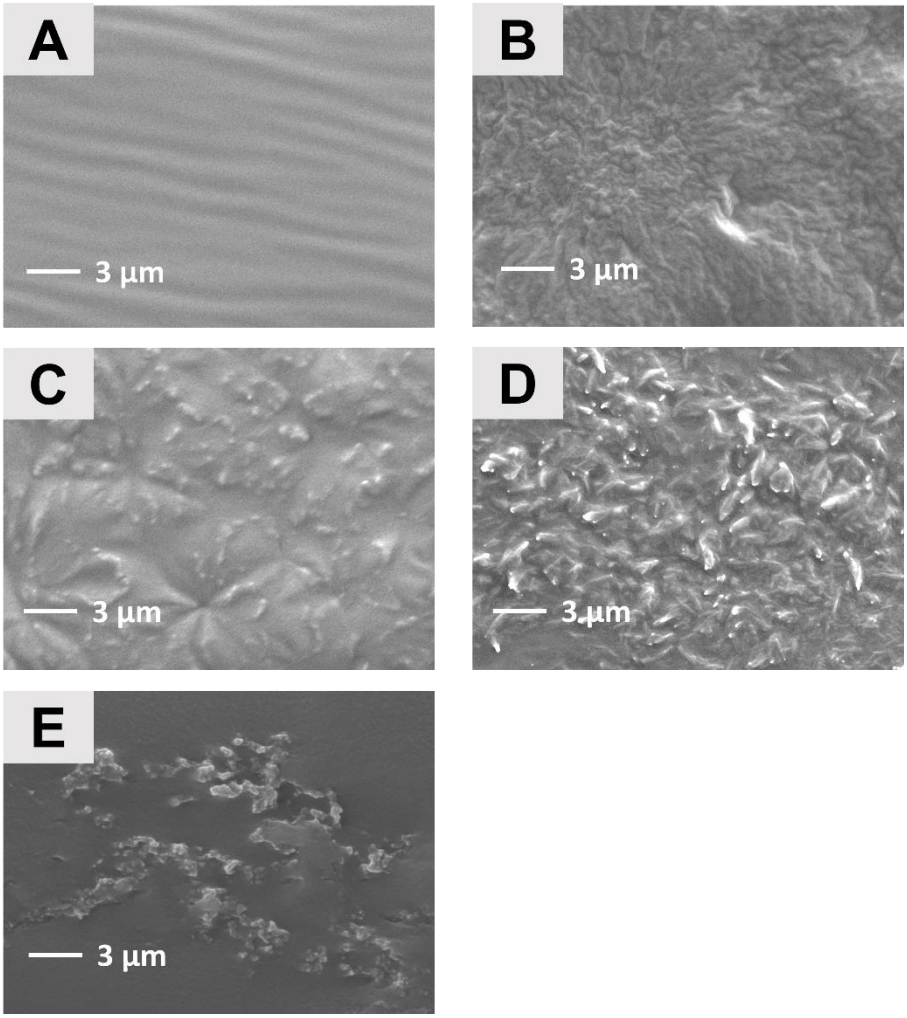

Fig. 3. Surface FESEM images of the ZIF-8@PDMS MMMs prepared without drying process: (A) ZIF-8@PDMS-0 (pristine PDMS membrane); (B) ZIF-8@PDMS-1 (1 wt% ZIF-8); (C) ZIF-8@PDMS-4 (4 wt% ZIF-8),(D) ZIF-8@PDMS-8 (8 wt% ZIF-8) and conventional (E) mZIF-8@PDMS-4 (4 wt% ZIF-8) MMM prepared with intermediate drying process.

Fig. 4

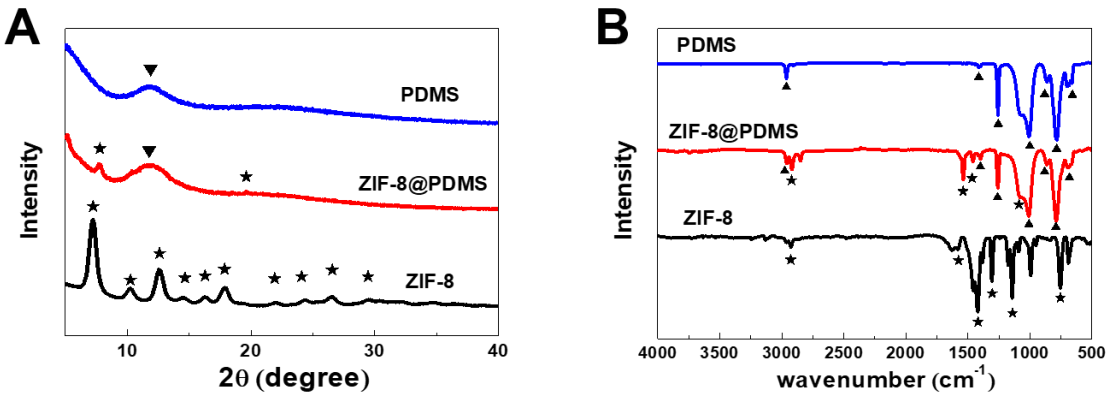

Fig. 4. (A) XRD and (B) FTIR patterns of pristine PDMS membrane, ZIF-8@PDMS-4 and pure ZIF-8 nanocrystals, where the ★ and ▲ representing the characteristic XRD or FTIR peaks of ZIF-8 and PDMS, respectively.

Fig. 5

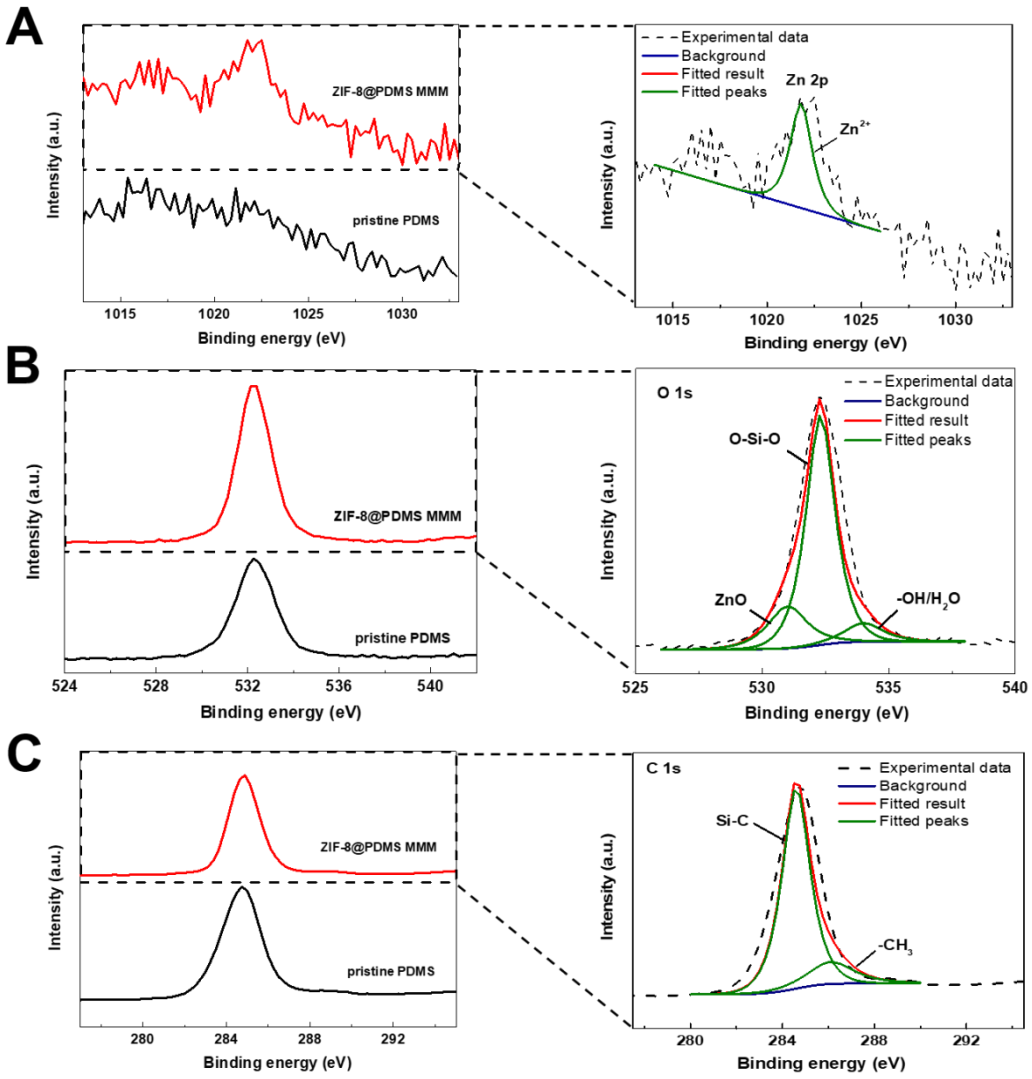

Fig. 5 The XPS characterization of (A) Zn 2p; (B) O 1s; and (C) C 1s on ZIF-8@PDMS-4 MMM and pristine PDMS membrane; and the corresponding curve fittings of ZIF-8@PDMS-4 MMM.

Fig. 6

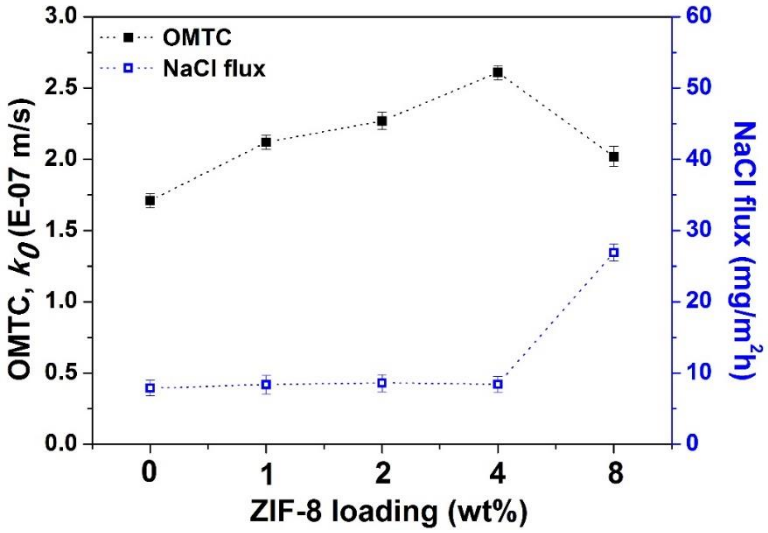

Fig. 6. The effect of ZIF-8 loadings (0, 1, 2, 4 and 8 wt%) on the aqueous-aqueous phenol extractive performance of ZIF-8@PDMS MMMs.

Fig. 7

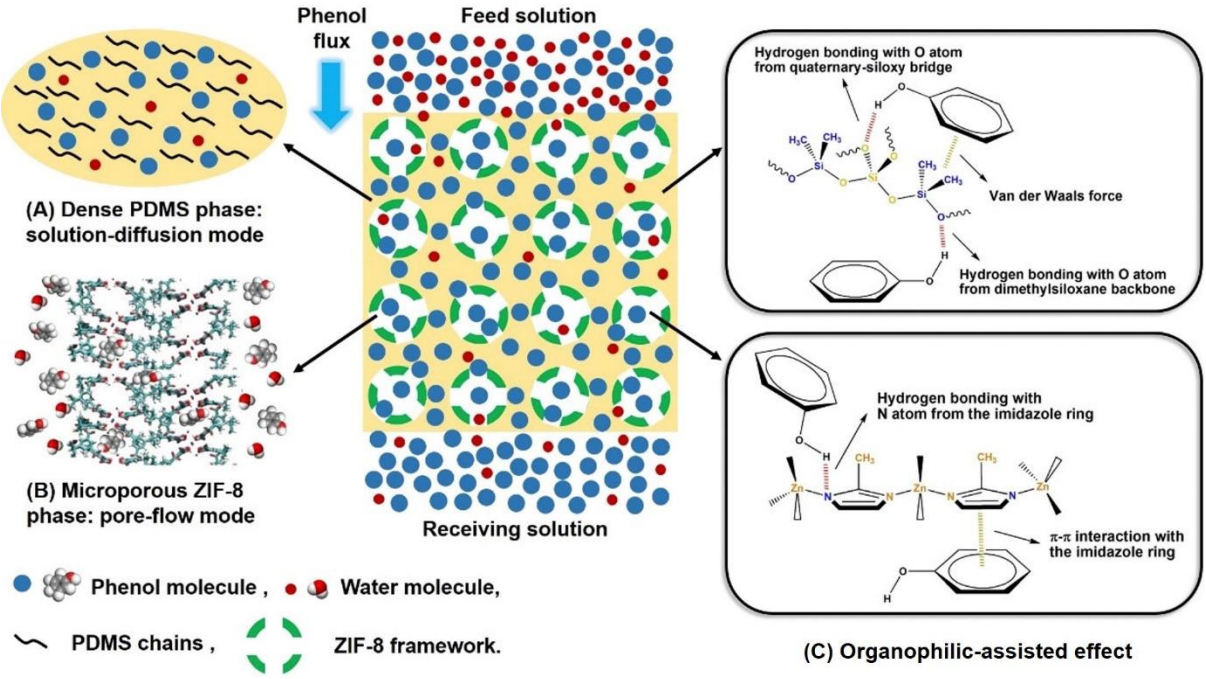

Fig. 7. Schematic diagram of an aqueous-aqueous phenol extractive process based on an organophilic-assisted "bi-mode" transport mechanism for a ZIF-8@PDMS MMM.

Fig. 8

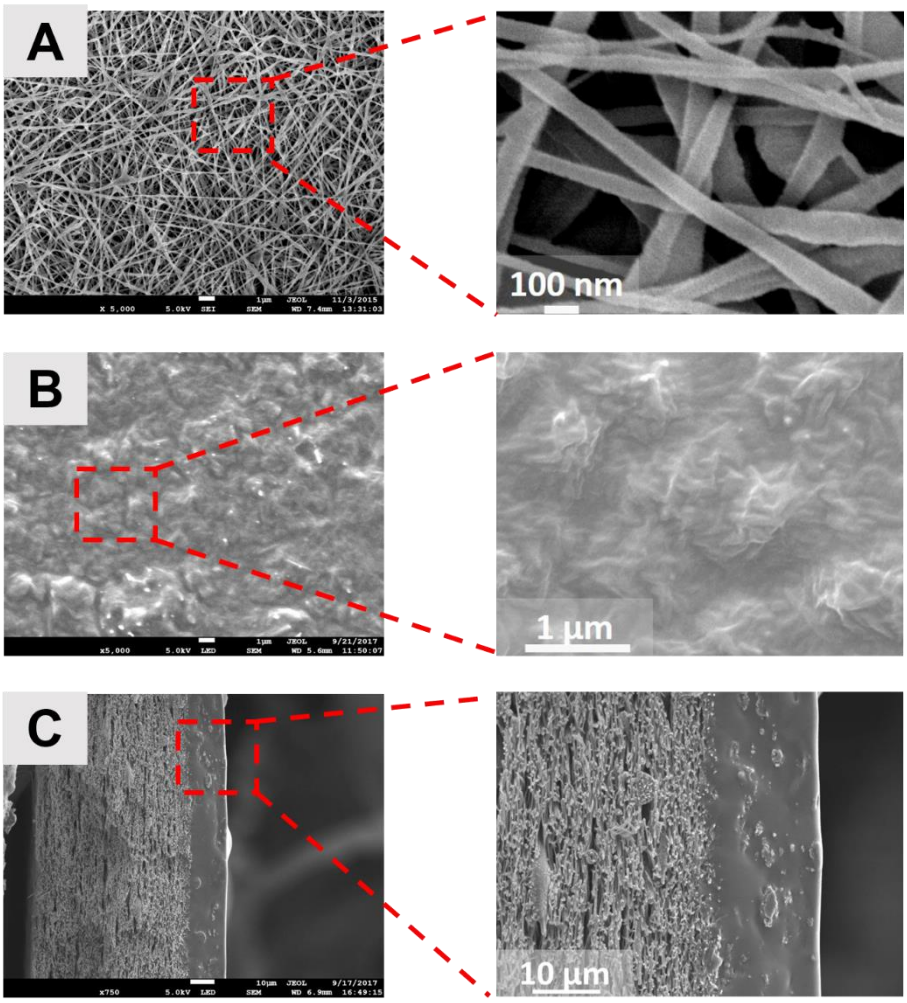

Fig. 8. Surface FESEM images of (A) a tiered PVDF electrospun nanofibrous support; (B) ZIF-8@PDMS-4/PVDF nanofibrous composite membrane M1; and (C) cross-sectional FESEM image of M1.

Fig. 9

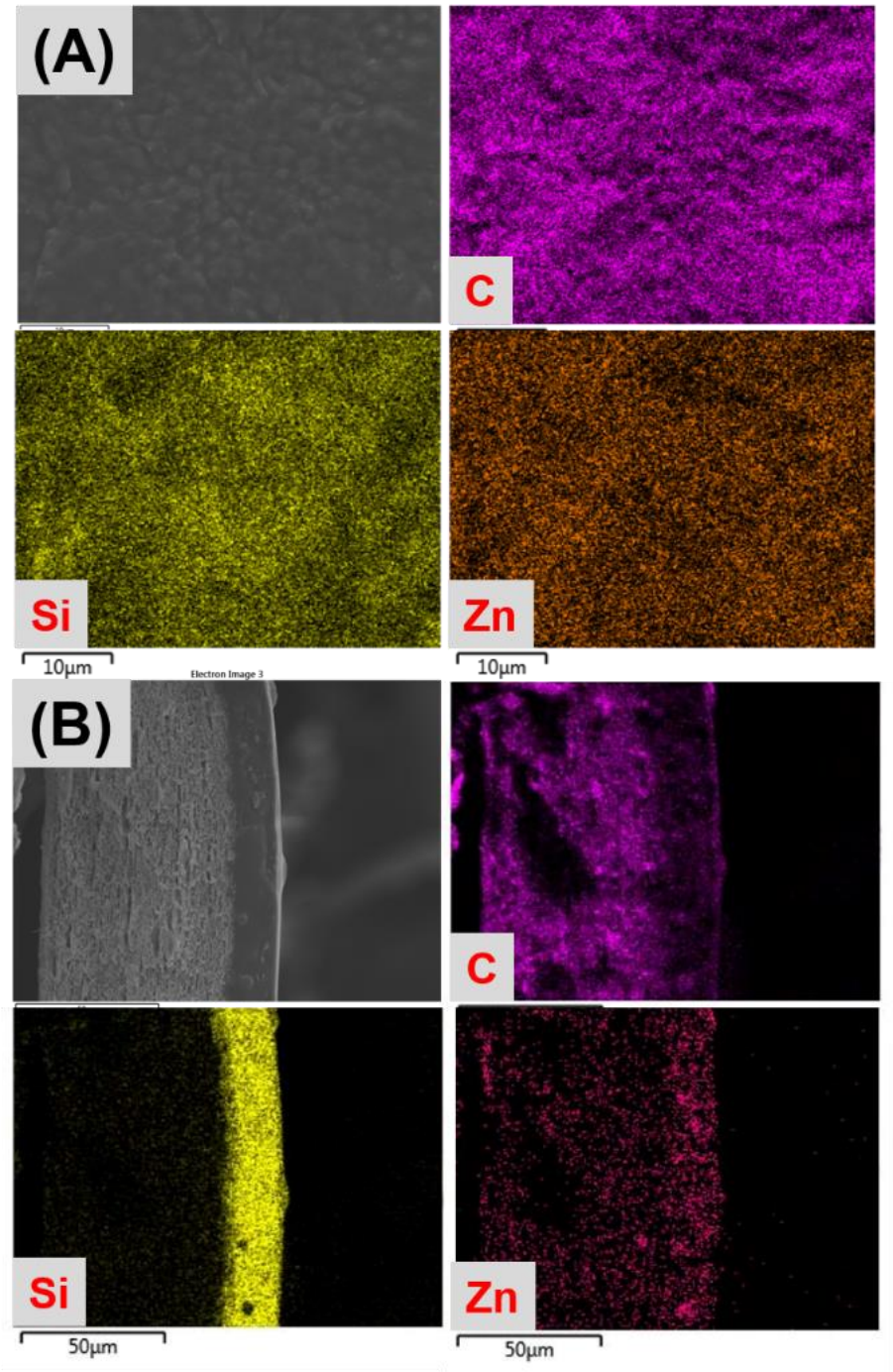

Fig. 9. (A) surface and (B) cross-sectional EDX analyses of ZIF-8@PDMS-4/PVDF nanofibrous composite membrane M1.

Fig. 10

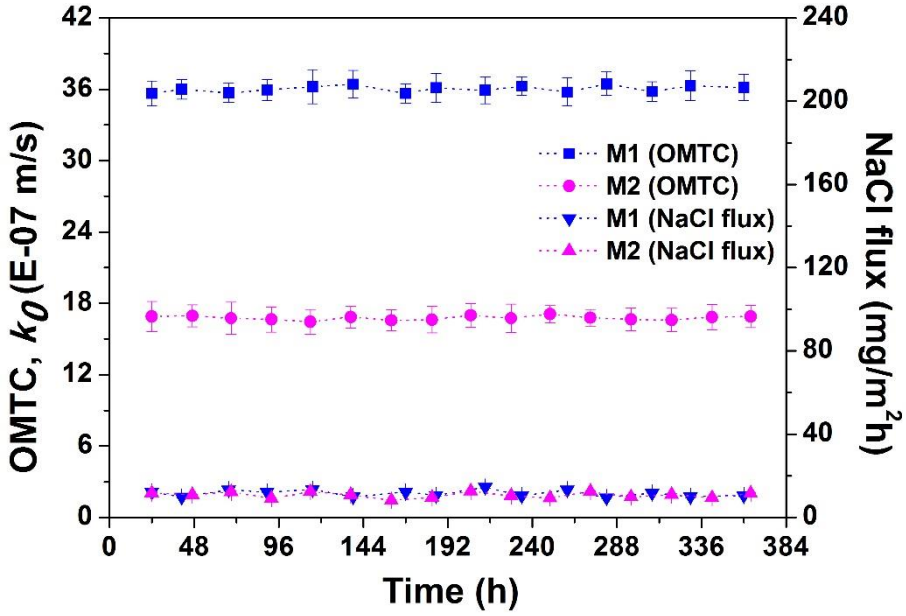

Fig. 10. Long-term performance of the nanofibrous composite membranes M1 and M2.

List of Tables

Table 1. Aqueous-aqueous phenol extractive performance of nanofibrous composite membranes.

Membrane Code	**Skin layer**	**Skin thickness (μm)**	k_0 **(E-07m/s)**	**NaCl flux (mg/m^{2}h)**
M1	ZIF-8@PDMS	13.2 ± 1.1	35.7 ± 1.1	12.3 ± 0.4
M2	PDMS	11.8 ± 0.9	16.9 ± 1.3	11.8 ± 0.4

Table 2. Comparison of aqueous-aqueous phenol extractive performance of various membranes.

Membrane type	**PDMS thickness (μm)**	**Substrate pore size (μm)**	**Feed solution condition**	**Reynolds number**	**OMTC, k_0 (E-07 m/s)**	**Reference**
#1 Tubular silicone rubber membrane	500	N.A.	1000 ppm phenol solution	12000 (feed side) 4700 (receiving side)	1.0	[14], 1995
#2 Tubular silicone rubber membrane	250	N.A.	1000 ppm phenol solution	12000 (feed side) 4700 (receiving side)	1.7	[14], 1995
#3 PDMS/PES TFC tubular membrane	2	0.1-10	phenol solution	7500 (feed side) 2700 (receiving side)	12	[17], 2002
#4 PDMS/PEI TFC-HF membrane	0.5-2	0.05	1000 ppm phenol, 50 g/L NaCl	1000 (both sides)	32	[18], 2016
#5 PDMS/PVDF nanofibrous composite membrane	55	0.3-0.6	1000 ppm phenol, 1 M HCl, 50 g/L NaCl	400 (both sides)	9.3	[10], 2017
#6 PDMS/PVDF nanofibrous composite membrane	7	0.3-0.6	1000 ppm phenol, 5 g/L NaCl	270 (both sides)	18	[19], 2018
#7 ZIF-8@PDMS/PVDF nanofibrous composite membrane	13	0.3-0.6	1000 ppm phenol, 5 g/L NaCl	300 (both sides)	36	Current work